not clear whether the catalytic action of the anion was concerted with the coordination of the nitrogen atom to the metal or if this coordination occurred after the methyl migration. In order to discriminate between these two possibilities we studied the distribution of the monolabeled products derived from the selected monolabeled complex **1a**.

In the presence of NBu_4I, complex **1a** isomerized and the equilibrium ^{13}C NMR spectrum showed the formation of complexes **1a**, **1b**, **2a**, and **2b**. Owing to the partial superimposition of the **1b** and **2a** bands, the ratio intensities **1a**:(**1b** + **2a**):**2b** = 0.9:1.9:1 were measured. On the basis of the equilibrium constant at 25 °C ($K = 1.2 \pm 0.1$), the ratios **1a**:**1b** and **2a**:**2b** are 1. The statistical formation of all possible monolabeled alkyl and dihaptoiminoacyl complexes indicates that the intermediate I can rotate before the coordination of the nitrogen atom (Scheme III). Therefore the catalytic action of the anion affects the methyl migration step: anions compel the methyl to migrate into the isocyanide carbon by either forming an ion pair[24] or by behaving as nucleophiles (as was observed recently for phosphine oxide[25]).

The thermodynamic stabilization of the η^2-iminoacyl structure is the drawing power of the reaction. The CO insertion does not occur because the η^2-acyl bond is less stable than the η^2-iminoacyl one.[4] This result agrees with Hoffmann's calculation,[1] which suggests that the isocyanide insertion can occur by stabilization due to the η^2-iminoacyl structure.

The isoelectronic ruthenium complex **5** reacts with halides, giving neutral complexes[26] $[Ru(CO)(PMe_3)_2(COCH_3)(CNR)X]$, and no insertion of isocyanide is observed. This is due to the more covalent character of the Ru-X bond with respect to iron.[27] Even when the anion has a low tendency to coordinate, such as NO_3^-, no isocyanide insertion is observed. This could be due to the stabilization of the alkyl with respect to the η^2-iminoacyl complex owing to less steric hindrance in the ruthenium complex.[28] Furthermore, no dynamic process is observed as is demonstrated by the absence of scrambling in the monolabeled **5a** complex in the presence of NBu_4NO_3.

In conclusion, the results of this work can be summarized as follows:

(a) The unsaturated intermediate (I) is dynamic and rearranges itself before the coordination of nitrogen.

(b) The anion catalysis operates only in the methyl migratory step.

(c) The CO insertion is easier than the CNR one;[8] in fact, in the presence of CO, the CO insertion is observed with the formation of complex **4**.

(d) The observation of isocyanide insertion in the absence of nucleophiles is due to the greater thermodynamic stability of the η^2-iminoacyl structure compared to the η^2-acyl one.

Acknowledgment. This work was supported by grants from the Consiglio Nazionale delle Ricerche (CNR, Rome, Italy) and the Ministero dell'Università e delle Ricerca Scientifica e Tecnlogica (MURST, Rome, Italy).

(24) Harned, H. S.; Owen, B. B. *The Physical Chemistry of Electrolytic Solutions*, 3rd ed.; Reinhold: New York, 1958.
(25) (a) Webb, S. L.; Giandomenico, C. M.; Halpern, J. *J. Am. Chem. Soc.* **1986**, *108*, 345-347. (b) Collman, J. P.; Hegedus, L. S.; Norton, J. R.; Finke, R. G. *Principles and Applications of Organotransition Metal Chemistry*, 2nd ed.; University Science Books: Mill Valley, CA, 1987; p 366.
(26) (a) Barnard, C. F. J.; Daniels, J. A.; Mawby, R. J. *J. Chem. Soc., Dalton Trans.* **1979**, 1331-1338. (b) Sanders, D. R.; Stephenson, M.; Mawby, R. J. *J. Chem. Soc., Dalton Trans.* **1984**, 1153-1156.
(27) (a) Pankowski, M.; Bigorgne, M. *J. Organomet. Chem.* **1977**, *125*, 231-252. (b) Barnard, C. F. J.; Daniels, J. A.; Jeffery, J.; Mawby, R. J. *J. Chem. Soc., Dalton Trans.* **1976**, 953-961.
(28) (a) Cotton, F. A.; Wilkinson, G. *Advanced Inorganic Chemistry*, 4th ed.; Wiley-Interscience: New York, 1980; pp 822-980. (b) Pitzer, K. S. *Acc. Chem. Res.* **1979**, *12*, 271-281.

Contribution from the Department of Chemistry, Baker Laboratory, Cornell University, Ithaca, New York 14853

Ketyl Complexes of $(silox)_3Ti$ (silox = $^tBu_3SiO^-$)

Katharine J. Covert, Peter T. Wolczanski,* Steven A. Hill,† and Paul J. Krusic†

Received June 25, 1991

Treatment of $TiCl_4(THF)_2$ or ZrX_4 (X = Cl, I) with 3.0 equiv of Na(silox) in THF afforded $(silox)_3TiCl$ (**1**, 85%) or $(silox)_3ZrX$ (X = Cl, **2**, 68%; I, **3**, 65%). According to electrochemical experiments, the reduction of **1**-**3** was feasible; orange, crystalline $(silox)_3Ti$ (**4**) was produced in 76% yield upon exposure of **1** to Na/Hg in DME, but a Zr(III) analogue could not be isolated. XPS data are used to rationalize the stability of low-valent siloxide complexes. UV-vis and EPR spectra of **4** were consistent with a D_{3h} geometry and $^2A_1'$ $(d_{z^2})^1$ ground state ($g_{iso} = 1.9554$, $g_{\parallel} = 1.9997$, $g_{\perp} = 1.9323$; $a_{iso} = 155$ MHz (~56.7 G)). Addition of L to **4** provided various thermally unstable adducts, $(silox)_3TiL$ (**4**-L; L = DME, CNMe, CN^{t}Bu, NC^{t}Bu, PMe_3, NH_3), whereas ketones and aldehydes reacted to give ketyls or compounds indicative of ketyl reactivity. Acetone and **4** produced a 1:1 mixture of $(silox)_3Ti(OCMe_2H)$ (**5a**) and $(silox)_3Ti(OMeC{=}CH_2)$ (**6a**), while acetaldehyde and **4** afforded a 1:1 mixture of $(silox)_3TiOEt$ (**5b**) and $(silox)_3TiOCH{=}CH_2$ (**6b**). Sterically hindered substrates (L = $^tBu_2CO$, ^tBuCHO, 3,3,5,5-tetramethylcyclohexanone, PhMeCO, 4,4'-dimethylbenzophenone) generated transient ketyls whose EPR spectra are indicative of carbon-centered radicals (**4**-OC^{t}Bu$_2$, $g = 1.9985$; **4**-OCH^{t}Bu, $g = 2.0001$; **4**-$OC_6H_6Me_4$, $g = 1.9920$; **4**-OCMePh, $g = 2.002$; **4**-OC(*p*-tolyl)$_2$, $g = 2.0005$). Benzophenone and **4** provided an equilibrium mixture of the ketyl $(silox)_3Ti(OCPh_2^{\bullet})$ (**4**-$OCPh_2$, $g = 2.0004$) and $[(silox)_3Ti(OCPh_2)]_2$ (**7**), which arises from a C_{α}-$C_{p\text{-Ph}}$ coupling reminiscent of trityl radical ($K_{eq}(25\ °C) = [\mathbf{4}\text{-}OCPh_2]^2/[\mathbf{7}] = 7.5 \times 10^{-7}$, $\Delta H_{diss} = 18$ (1) kcal/mol, $\Delta S = 33$ (3) eu). Addition of Ph_3SnH to **7** yielded $(silox)_3TiOCPh_2H$ (**8**) and $Ph_3SnSnPh_3$. Ketyl formation was also reversible, since addition of 4,4'-dimethylbenzophenone to **7** produced some of the mixed diarylketone dimer $(silox)_3Ti\text{-}O(tolyl)_2\overline{C(H)C(CH)_2C(CH{=}CH)}{=}C(Ph)OTi(silox)_3$ (**9**). EPR studies of **4**-OCRR' were clearly supportive of the ketyl formulation; tentative evidence for a chair ⇌ chair interconversion in **4**-$OC_6H_6Me_4$ and equilibration of the Ph rings in **4**-$OCPh_2$ is also presented. The EPR and UV-vis spectra of **4** are rationalized in terms of a relatively strong ligand field. The *g* values and hyperfine couplings of the ketyls are used to assess the binding of the R'RC=O substrates, and sterics play the major role.

Introduction

Applications of inorganic and organometallic reagents to organic synthesis comprise an active and productive area of chemical research.[1-3] The stabilization and isolation of inherently reactive organic fragments through binding to transition-metal centers is

(1) Collman, J. P.; Hegedus, L. S.; Norton, J. R.; Finke, R. G. *Principles and Applications of Organotransition Metal Chemistry*; University Science Books: Mill Valley, CA, 1987.
(2) Negishi, E. I. *Organometallics in Organic Synthesis*; Wiley-Interscience: New York, 1980.

† Present address: E. I. du Pont de Nemours & Co., Inc., Central Research and Development, Experimental Station, Wilmington, DE 19898.

0020-1669/92/1331-0066$03.00/0

often a fundamentally interesting component of these efforts. Recent use of radical cyclizations as synthetic methods[4,5] has prompted a renewed interest in the application of paramagnetic organometallic complexes, particularly those containing d^1 electronic configurations. Nugent and RajanBabu[6] have used oxophilic Ti(III) derivatives to generate radicals via the ring-opening of epoxides, and Pedersen has uncovered novel reagents for the cross-coupling of carbonyl compounds and imines.[7,8]

Consider the prototypical pinacol reaction

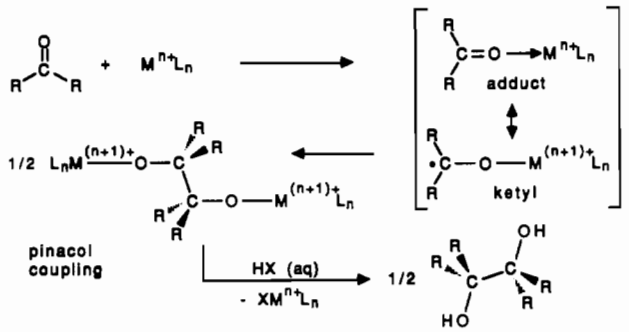

where reduction of a carbonyl functionality results in carbon–carbon bond formation. In this sequence, the carbonyl adduct can be construed as a ketyl complex, since the ensuing chemistry is indicative of radical coupling, and alkali-metal species have been shown to possess substantial electron density (~70%) on carbon.[9] Heterogeneous reagents such as $TiCl_4/Mg$,[10] $VCl_3/Mg/^tBuOH$,[11] and Ce/I_2[12] are commonly used to effect pinacol couplings of aldehydes and ketones,[13] whereas organometallic titanium[14,15] and vanadium[16] complexes have been studied as homogeneous analogues[17] to these relatively ill-defined systems. Furthermore, pinacolates are important intermediates in the reductive coupling of organic carbonyls to olefins, the McMurry reaction.[18] The McMurry reagent, formed in situ from $TiCl_3$ and a reducing agent such as Li^0, $LiAlH_4$, or Cu/Zn, has been used to form carbon–carbon double bonds in a number of natural products and strained carbocycles.[19]

While several pinacolate-bridged dimetallic compounds have been isolated, including Caulton's structurally characterized $(CpCl_2Ti)_2(\mu\text{-}O_2C_2Me_4)$,[20] transition-metal ketyl species (i.e., $L_nM\text{–}OCR_2^{\bullet}$) are rare. For oxophilic, d^0 early-transition-metal complexes, coordination of organic carbonyls often occurs via an oxygen lone pair,[21-23] but no reduction can occur. In contrast, d^n ($n \geq 2$) metal centers tend to bind ketones and aldehydes in an η^2-mode. For example, Chisholm has recently shown that an η^2-$OCPh_2$ complex precedes formation of a mononuclear pinacolate, $(RO)_4W(O_2C_2Ph_4)$.[24] In an accompanying study, $(^tBuCH_2O)_6W_2(py)_2$ was shown to reductively cross-couple certain ketones and aldehydes, but the transformation occurs via binuclear alkylidene-bridged, μ-oxo intermediates[25] and not through a pinacolate. A similar mononuclear cleavage of cyclopentanone by $(Ph_2MeP)_4Cl_2W$ to give $(Ph_2MeP)_2Cl_2(O{=})W{=}C(CH_2)_3CH_2$ was observed by Mayer.[26] Curiously, treatment of the W(II) complex with benzophenone generated an η^1-$OCPh_2$ complex, followed by $Ph_2C{=}CPh_2$ loss akin to a McMurry coupling reaction, a result rationalized on the basis of sterics. In accord with these observations, dinuclear pinacolates have been stabilized upon addition of certain ketones to ditungsten(IV) alkoxide complexes.[27]

Despite these recent synthetic and mechanistic explorations into the reductive coupling of organic carbonyls, observation of a transition-metal ketyl remained elusive. When treated with ketones and aldehydes, oxophilic d^1 complexes rapidly produced pinacolates; thus the putative intermediate ketyls were presumed to be highly reactive.[14-17,20] In this investigation, a sterically encumbered d^1 center, $(silox)_3Ti$ ($silox^{28,29}$ = $^tBu_3SiO^-$), was employed to slow the carbon–carbon bond-forming step subsequent to ketyl formation. Previous work has shown that the peripheral hydrocarbon shell of a tris(silox) coordination sphere is an effective steric shield[30-33] and that the electron is transposed from Ti to

(3) Reetz, M. T. *Organotitanium Reagents in Organic Synthesis*; Springer-Verlag: New York, 1986.
(4) (a) Stork, G. In *Current Trends in Organic Synthesis*; Nozaki, H., Ed.; Pergamon Press: Oxford, England, 1983. (b) Hart, D. J. *Science (Washington, D.C.)* **1984**, *223*, 883–887.
(5) (a) Stork, G.; Sher, P. M. *J. Am. Chem. Soc.* **1986**, *108*, 303–304. (b) Meijs, G. F.; Beckwith, A. L. J. *Ibid.* **1986**, *108*, 5890–5893. (c) Beckwith, A. L. J.; Roberts, D. H. *Ibid.* **1986**, *108*, 5893–5901.
(6) (a) RajanBabu, T. V.; Nugent, W. A.; Beattie, M. S. *J. Am. Chem. Soc.* **1990**, *112*, 6408–6409. (b) RajanBabu, T. V.; Nugent, W. A. *Ibid.* **1989**, *111*, 8561–8562. (c) RajanBabu, T. V.; Nugent, W. A. *Ibid.* **1988**, *110*, 4525–4527.
(7) Freudenberger, J. W.; Konradi, A. W.; Pedersen, S. F. *J. Am. Chem. Soc.* **1989**, *111*, 8014–8016.
(8) (a) Roskamp, E. J.; Pedersen, S. F. *J. Am. Chem. Soc.* **1987**, *109*, 3152–3154. (b) Roskamp, E. J.; Pedersen, S. F. *Ibid.* **1987**, *109*, 6551–6553.
(9) (a) March, J. *Advanced Organic Chemistry*, 3rd ed.; Wiley: New York, 1985. (b) Seebach, D.; Weidmann, B.; Widler, L. In *Modern Synthetic Methods*; Scheffold, R., Ed.; John Wiley & Sons: New York, 1983; Vol. 3, pp 290–298. (c) House, H. O. *Modern Synthetic Reactions*, 2nd ed.; W. A. Benjamin: New York, 1972, and references therein.
(10) Corey, E. J.; Danheiser, R. L.; Chandrasekaran, S. *J. Org. Chem.* **1976**, *41*, 260–265.
(11) Pons, J. M.; Zahra, J. P.; Santelli, M. *Tetrahedron Lett.* **1981**, *22*, 3965–3968.
(12) Imamota, T.; Kusomota, T.; Hatanaka, Y.; Yokoyama, M. *Tetrahedron Lett.* **1982**, *23*, 1353–1356.
(13) For a general overview of carbonyl couplings, see: Kahn, B. E.; Riecke, R. T. *Chem. Rev.* **1988**, *88*, 733–745.
(14) Coutts, R. S. P.; Wailes, P. C.; Martin, R. L. *J. Organomet. Chem.* **1973**, *50*, 145–151.
(15) (a) Klei, E.; Telgen, J. H.; Teuben, J. H. *J. Organomet. Chem.* **1981**, *209*, 297–307. (b) Teuben, J. H.; DeBoer, E. J. M.; Klazinga, A. H.; Klei, E. *J. Mol. Catal.* **1981**, *13*, 107–114.
(16) (a) Gambarotta, S.; Floriani, C.; Chiesi-Villa, A.; Guastini, C. *Organometallics* **1986**, *5*, 2425–2433. (b) Floriani, C. *Pure Appl. Chem.* **1982**, *54*, 59–64.
(17) For a brief overview, see: Bottrill, M.; Gavens, P. D.; Kelland, J. W.; McMeeking, J. In *Comprehensive Organometallic Chemistry*; Wilkinson, G., Stone, F. G. A., Abel, E. W., Eds.; Pergamon: New York, 1982; Vol. 3, pp 273–274.
(18) (a) McMurry, J. E. *Acc. Chem. Res.* **1983**, *16*, 405–411. (b) Dams, R.; Malinowski, M.; Westdorp, I.; Geise, H. *J. Org. Chem.* **1982**, *47*, 248–259.
(19) McMurry, J. E. *Chem. Rev.* **1989**, *89*, 1513–1524.
(20) Huffman, J. C.; Moloy, K. G.; Marsella, J. A.; Caulton, K. G. *J. Am. Chem. Soc.* **1980**, *102*, 3009–3014.
(21) (a) McAuliffe, C. A.; Barratt, P. S. In *Comprehensive Coordination Chemistry*; Wilkinson, G., Gillard, R. D., McCleverty, J. A., Eds.; Pergamon: New York, 1987; Vol. 3, Chapter 31. (b) Fay, R. C. In *Comprehensive Coordination Chemistry*; Wilkinson, G.; Gillard, R. D.; McCleverty, J. A., Eds.; Pergamon: New York, 1987; Vol. 3, Chapter 32.
(22) For structural information on titanium and zirconium ketone and ester adducts, see: (a) Galeffi, B.; Simard, M.; Wuest, J. D. *Inorg. Chem.* **1990**, *29*, 951–954. (b) Maier, G.; Seipp, U. *Tetrahedron Lett.* **1987**, *28*, 4515–4516. (c) Utko, J.; Sobata, P.; Lis, T. *J. Organomet. Chem.* **1987**, *334*, 341–345.
(23) For a brief survey of carbonyl complexation critical to some organic transformations, see: (a) Reetz, M. T.; Hüllmann, M.; Seitz, T. *Angew. Chem., Int. Ed. Engl.* **1987**, *26*, 477–479. (b) Keck, G. E.; Castellino, S. *J. Am. Chem. Soc.* **1986**, *108*, 3847–3849. (c) Poll, T.; Metter, J. O.; Helmchen, G. *Angew. Chem., Int. Ed. Engl.* **1985**, *24*, 112–114. (d) Bassi, I. W.; Calcaterra, M.; Intrito, R. *J. Organomet. Chem.* **1977**, *127*, 305–315.
(24) Chisholm, M. H.; Folting, K.; Klang, J. A. *Organometallics* **1990**, *9*, 607–613.
(25) (a) Chisholm, M. H.; Klang, J. A. *J. Am. Chem. Soc.* **1989**, *111*, 2324–2325. (b) Chisholm, M. H.; Folting, K.; Klang, J. A. *Organometallics* **1990**, *9*, 602–606.
(26) (a) Bryan, T. C.; Mayer, J. M. *J. Am. Chem. Soc.* **1990**, *112*, 2298–2308. (b) Bryan, T. C.; Mayer, J. M. *Ibid.* **1987**, *107*, 7213–7214. (c) Su, F.-M.; Bryan, J. M.; Jang, S.; Mayer, J. H. *Polyhedron* **1989**, *8*, 1261–1267.
(27) (a) Anderson, L. B.; Cotton, F. A.; DeMarco, D.; Falvello, L. R.; Tetrick, S. M.; Walton, R. A. *J. Am. Chem. Soc.* **1984**, *106*, 4743–4749. (b) Cotton, F. A.; DeMarco, D.; Falvello, L. R.; Walton, R. A. *Ibid.* **1982**, *104*, 7375–7376.
(28) (a) Weidenbruch, M.; Pierrard, C.; Pesel, H. *Z. Naturforsch. B: Anorg. Chem., Org. Chem.* **1978**, *33B*, 1468–1471. (b) Dexheimer, E. M.; Spialter, L.; Smithson, L. D. *J. Organomet. Chem.* **1975**, *102*, 21–27.
(29) LaPointe, R. E.; Wolczanski, P. T.; Van Duyne, G. D. *Organometallics* **1985**, *4*, 1810–1818.
(30) Neithamer, D. R.; LaPointe, R. E.; Wheeler, R. A.; Richeson, D. A.; VanDuyne, G. D.; Wolczanski, P. T. *J. Am. Chem. Soc.* **1989**, *111*, 9056–9072.

4

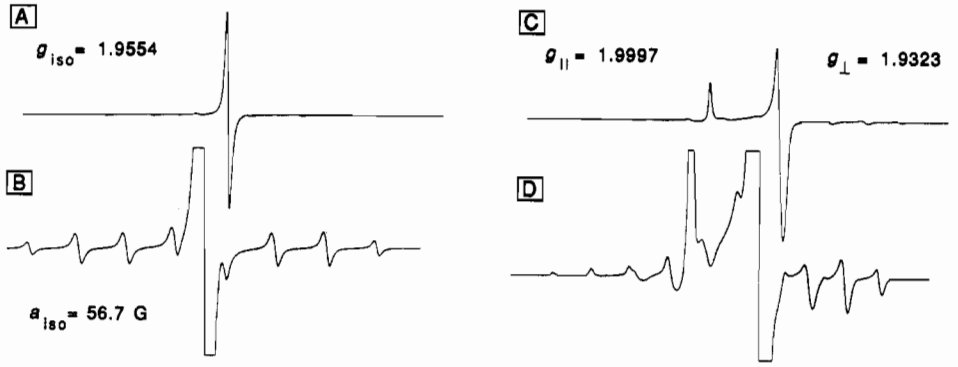

Figure 1. EPR spectra of $(silox)_3Ti$ (**4**) in toluene solution (A, B; 298 K) and glass (C, D; 106 K).

the carbonyl carbon of a benzophenone ligand.[33] Reported herein are various ketyl complexes of $(silox)_3Ti$, as characterized by EPR spectroscopy.

Results

Synthetic Studies. Treatment of $TiCl_4(THF)_2$[34] with 3.0 equiv of Na(silox) in refluxing THF for 12–15 h provided colorless $(silox)_3TiCl$ (**1**) in 85% yield (eq 1). In contrast to the titanium complex, tris(silox)zirconium halides formed smoothly in THF at 25 °C (eq 2), and no intermediate mono- or bis(silox) intermediates were observed when the reaction was monitored by ^1H NMR spectroscopy. Crystallization from hexanes afforded $(silox)_3ZrX$ (X = Cl (**2**), I (**3**)) in 68% and 65% yields, respectively. Both compounds were stable in C_6D_6 solution at 200 °C for >3 days, and each melted without noticeable decomposition (**2**, 295–298 °C; **3**, 105–107 °C), thereby exhibiting the robust character of silox halides previously observed.[28,29]

$$3Na(silox) + TiCl_4(THF)_2 \xrightarrow[12\text{–}15\ h]{THF,\ 70\ °C} \underset{\mathbf{1}}{(silox)_3TiCl} + 3NaCl \quad (1)$$

$$3Na(silox) + ZrX_4 \xrightarrow[12\text{–}15\ h]{THF,\ 25\ °C} \underset{\begin{array}{c}X = Cl\ (\mathbf{2})\\ X = I\ (\mathbf{3})\end{array}}{(silox)_3ZrX} + 3NaCl \quad (2)$$

Cyclic voltammograms of **1** and **2**, recorded in THF with $^nBu_4NBF_4$ as electrolyte, suggested that the reduction of each was feasible. $(silox)_3TiCl$ (**1**) showed an electrochemically irreversible reduction at −1.10 V (Ag/AgCl; ΔE_p = 270 mV, 130 mV for Cp_2Fe/Cp_2Fe^+), while $(silox)_3ZrCl$ (**2**) manifested a similar wave at −1.8 V. Since these survey experiments implicated a fast step subsequent to electrochemical electron transfer (eq 3),[35] the reduction chemistry of **1**–**3** was pursued.

$$(silox)_3MCl \xrightarrow{+e^-} [(silox)_3MCl^-] \xrightarrow{fast} [(silox)_3M] + Cl^- \quad (3)$$
M = Ti (**1**)
M = Zr (**2**)

Exposure of $(silox)_3ZrCl$ (**2**) or $(silox)_3ZrI$ (**3**) to Na/Hg, Na(naphthalenide), and Na^0 in various ethereal and hydrocarbon solvents provided little or no evidence of reduction. Similar attempts with Na/K alloy or Cs^0 led to transiently colored solutions (red to brown), which quickly decomposed into a multitude of uncharacterized products. Efforts to scavenge transient Zr(III) species by conducting the reductions under PMe_3, N_2, CO, or H_2 failed to yield identifiable derivatives. Since a Ti(III) complex was expected to be both thermodynamically and kinetically more stable than the heavier group 4 congeners, the reduction of **1** was considered.

When $(silox)_3TiCl$ (**1**) was subjected to Na/Hg in DME, the initially colorless solution turned green-brown over the course of 3–4 h due to the formation of light green $(silox)_3Ti(DME)$ (**4**–DME, eq 4). The DME was labile and could be liberated by dissolution in toluene or heptane, followed by removal of the solvent (eq 5). Orange $(silox)_3Ti$ (**4**) was crystallized from hexanes in 76% yield. The use of DME was crucial, since reductions in THF and Et_2O led to degradation[36] and those in hydrocarbon media were complicated by the formation of an insoluble yellow powder.

$$\underset{\mathbf{1}}{(silox)_3TiCl} \xrightarrow[DME]{Na/Hg,\ -NaCl} \underset{\mathbf{4}\text{–DME}}{(silox)_3Ti(DME)} \quad (4)$$

$$\mathbf{4}\text{–DME} \xrightarrow[toluene]{} \underset{\mathbf{4}}{(silox)_3Ti} + DME\uparrow \quad (5)$$

Characterization of $(silox)_3Ti$ (4). While attempts to determine the structure of $(silox)_3Ti$ (**4**) by X-ray crystallography were thwarted by crystal twinning, cryoscopic molecular weight measurements indicated that **4** was monomeric (M_r: found, 709; calcd, 694), consistent with a trigonal planar (D_{3h}) geometry. The UV–vis spectrum of d^1 **4** consisted of a symmetrical d–d band ($^2A' \rightarrow {}^2E'$, $(d_{z^2})^1 \rightarrow (d_{x^2-y^2}, d_{xy})^1$) at 500 nm (20 000 cm^{-1}, ϵ = 360 $M^{-1}\ cm^{-1}$) and two intense absorptions at 248 nm (40 320 cm^{-1}, ϵ = 13 600 $M^{-1}\ cm^{-1}$) and 211 nm (47 390 cm^{-1}, ϵ = 15 000), assigned as LMCT and intraligand bands, respectively.[32] No electronic transitions were observed in the near-infrared region.

The paramagnetic complex (μ = 2.0 μ_B) exhibited a broad resonance at δ 1.5 ($\upsilon_{1/2}$ = 110 Hz) in the ^1H NMR spectrum, but no resonances were detected by $^{13}C\{^1H\}$ NMR spectroscopy. The 25 °C EPR spectrum of **4** (Figure 1A,B) revealed a single absorption with an isotropic g_{iso} = 1.9554, indicative of a titanium-centered radical.[37–39] Hyperfine couplings to ^{47}Ti ($S = {}^5/_2$, 7.5%) and ^{49}Ti ($S = {}^7/_2$, 5.5%) were superimposed as six- and eight-line patterns with an isotropic a_{iso} = 155 MHz (~56.7 G).

(31) (a) LaPointe, R. E.; Wolczanski, P. T. *J. Am. Chem. Soc.* **1986**, *108*, 3535–3537. (b) Toreki, R.; LaPointe, R. E.; Wolczanski, P. T. *Ibid.* **1987**, *109*, 7558–7560.
(32) Covert, K. J.; Neithamer, D. R.; Zonnevylle, M. C.; LaPointe, R. E.; Schaller, C. P.; Wolczanski, P. T. *Inorg. Chem.* **1991**, *30*, 2494–2508.
(33) A preliminary account of the benzophenone chemistry has been reported. Covert, K. J.; Wolczanski, P. T. *Inorg. Chem.* **1989**, *28*, 4565–4567.
(34) Manzer, L. *Inorg. Synth.* **1982**, *21*, 135–140.
(35) Bard, A. J.; Faulkner, L. R. *Electrochemical Methods: Fundamentals and Applications*; John Wiley and Sons: New York, 1980.
(36) Covert, K. J. Ph.D. Thesis, Cornell University, 1990.
(37) Wertz, J. E.; Bolton, J. R. *Electron Spin Resonance*; Chapman and Hall: New York, 1986.
(38) Abragam, A.; Bleaney, B. *Electron Paramagnetic Resonance of Transition Ions*; Clarendon: New York, 1970.
(39) Gordy, W. *Theory and Applications of Electron Spin Resonance*; Wiley-Interscience: New York, 1980.

Scheme I

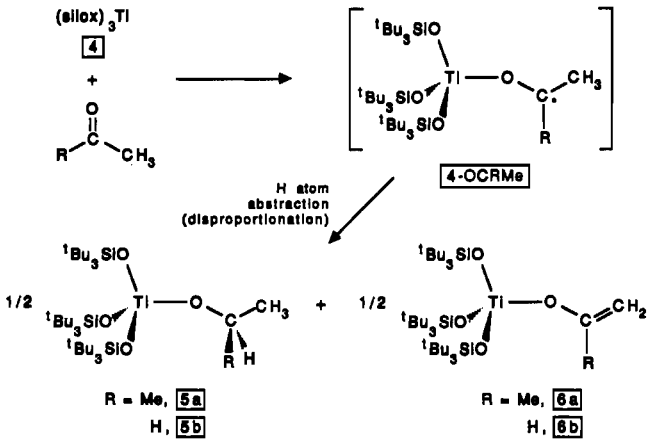

The powder spectrum of **4**, taken in toluene at 77 K (Figure 1C,D), characterized an axially symmetric molecule with $g_\parallel = 1.9997$, $g_\perp = 1.9323$ and accompanying hyperfine couplings of $a_\parallel = 171$ MHz (~61.2 G) and $a_\perp = \sim 153$ MHz (~56.8 G), although the latter was difficult to measure. From the isotropic hyperfine coupling of 155 MHz and the more easily measured $a_\parallel$, $a_\perp$ may actually approach 147 MHz ($\{2a_\perp + a_\parallel\}/3 = a_{iso}$), assuming that the **a** and **g** tensors are coincident.

Attempts to electrochemically oxidize $(silox)_3Ti$ (**4**) were prone to interference from the anions of available electrolytes (i.e., BF_4^-, BPh_4^-, and PF_6^-), resulting in rapid decomposition and ambiguous results. Chemical oxidants (Cp_2Fe^+ and Ag^+) also failed to yield the desired cationic species, $[(silox)_3Ti]^+$, presumably due to the same constraints. This undesired reactivity with common anions (e.g., F^- abstraction), in combination with the instability of **4** in most solvents used for electrochemistry (e.g., THF,[40] CH_2Cl_2), precluded further oxidation efforts.

Adducts of $(silox)_3Ti$ (4). Coordinatively unsaturated $(silox)_3Ti$ (**4**) was observed to bind various Lewis bases in forming pale green, pseudotetrahedral adducts, $(silox)_3TiL$ (**4**–L; L = DME, CNMe, CN^{t}Bu, NC^{t}Bu, PMe_3, NH_3; eq 6). Larger ligands such as PPh_3

$$(silox)_3Ti + L \rightarrow (silox)_3Ti\text{–}L \qquad (6)$$
$$\mathbf{4} \qquad\qquad \mathbf{4}\text{–}L$$

L = DME, CNMe, CN^{t}Bu, NC^{t}Bu, PMe_3, NH_3

did not bind to the sterically hindered Ti(III) site, while PMe_3 and ammonia were weakly bound and readily removed in dynamic vacuum. The remaining complexes also lost L when heated and were stored at −30 °C as a precaution. Light green solutions were also observed after the addition of THF, diethyl ether, or H_2O to $(silox)_3Ti$ (**4**), but these presumed adducts were only transiently stable[40] and no characterization was attempted. All of the ligands, even those with good π-accepting capability, appear to be functioning merely as σ-donors. For example, the ν(C≡N) bands of **4**–CNMe and **4**–CN^{t}Bu were observed at 2209 and 2250 cm^{-1}, respectively; these stretching frequencies are substantially higher than those for the corresponding free ligands (CNR: R = Me, 2130 cm^{-1}; R = ^{t}Bu, 2133 cm^{-1}). In addition, the 2246-cm^{-1} band observed for ν(N≡C) of pivalonitrile adduct **4**–NC^{t}Bu is near that of the free ligand value (2250 cm^{-1}). No EPR signals were observed for any of the adducts, either at 25 °C or as powder samples in 2-methylpentane at 77 K.

Ketyl Derivatives of $(silox)_3Ti$ (4). As Scheme I indicates, the reaction of $(silox)_3Ti$ (**4**) with OCRMe (R = Me, H) afforded product mixtures commensurate with the formation of ketyl intermediates. Acetone and **4** combined to generate isopropoxide $(silox)_3Ti(OCMe_2H)$ (**5a**) and 2-propenyl oxide $(silox)_3Ti(OMeC{=}CH_2)$ (**6a**) in a 1:1 ratio, while acetaldehyde reacted with **4** to give a 1:1 mixture of ethoxide $(silox)_3TiOEt$ (**5b**) and enolate $(silox)_3TiOCH{=}CH_2$ (**6b**). In contrast to the isocyanide adducts that exhibited minimal π-back-bonding, these products are consistent with the transposition of an electron from Ti to the carbonyl carbon of each substrate. In essence, the intermediate adduct exhibited Ti(IV) (i.e., $(silox)_3Ti^{IV}OCRMe^\bullet$) rather than Ti(III) (i.e., $(silox)_3Ti^{III}O{=}CRMe$) character. Once formed, the ketyl degraded to the alkoxide and enoxide moieties by H atom transfer pathways reminiscent of *tert*-butyl radical disproportionation to isobutane and isobutylene.[41] In contrast to ^{t}Bu$^\bullet$, coupling of the ketyls was not observed, perhaps due to the sizable bulk of the $(silox)_3Ti$ center.

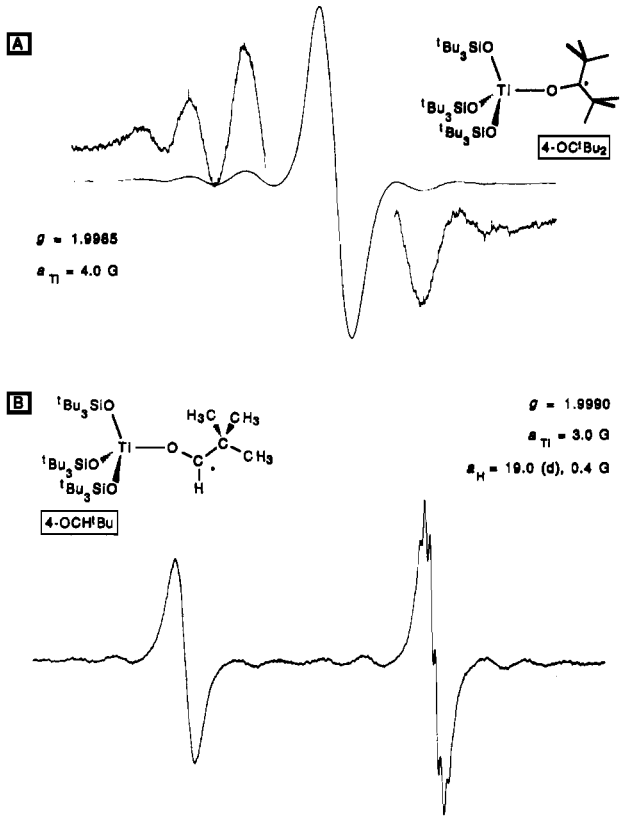

Figure 2. EPR spectra (toluene) of $(silox)_3TiOC^tBu_2^\bullet$ (**4**–OC^{t}Bu$_2$) at 213 K (A) and $(silox)_3TiOCH^tBu^\bullet$ (**4**–OCH^{t}Bu) at 203 K (B). The latter manifests anisotropy in the signal as indicated by the slow-motion broadening of the lower field line.

Stabilization of the transient ketyl was sought through inhibition of two prominent radical decomposition pathways, H atom transfer and R$^\bullet$ coupling.[41] Sterically protected carbonyl species devoid of β-hydrogens were considered substrates capable of forming ketyl species. An orange solution containing $(silox)_3Ti$ (**4**) and di-*tert*-butyl ketone became ink blue at temperatures below 0 °C, indicating a reversible equilibrium with $(silox)_3Ti(OC^tBu_2^\bullet)$ (**4**–OC^{t}Bu$_2$) (eq 7). Accompanying the color change was a new EPR

$$(silox)_3Ti + O{=}C^tBu_2 \rightleftharpoons (silox)_3Ti\text{—}O\text{—}C^tBu_2^\bullet \qquad (7)$$
$$\mathbf{4} \qquad\qquad \mathbf{4}\text{–}OC^tBu_2$$

signal corresponding to **4**–OC^{t}Bu$_2$, centered at $g = 1.9985$ with an isotropic titanium (^{47,49}Ti) hyperfine coupling of $a_{iso} = 4$ G (Figure 2A).[42] A weak doublet tentatively assigned to **4**–O^{13}C^{t}Bu$_2$ (1.1%, $a_c \sim 26$ G) was barely observed.

With pivaldehyde as the substrate, the dark blue solution formed upon mixing, presumably due to formation of $(silox)_3Ti(OCH^tBu^\bullet)$ (**4**–OCH^{t}Bu, eq 8). At 203 K, the EPR spectrum of **4**–OCH^{t}Bu

$$(silox)_3Ti + O{=}CH^tBu \rightleftharpoons (silox)_3Ti\text{—}O\text{—}CH^tBu^\bullet \qquad (8)$$
$$\mathbf{4} \qquad\qquad \mathbf{4}\text{–}OCH^tBu$$

displayed a doublet centered at $g = 1.9990$ due to coupling (a_H

(40) $(silox)_3Ti$ (**4**) has been shown to cleave THF: Covert, K. J.; Wolczanski, P. T. Unpublished results.

(41) Kochi, J. *Free Radicals*; Wiley: New York, 1973.

(42) For the EPR of $^tBu_2CO$ radical anion, see: Hirota, N.; Weissman, S. I. *J. Am. Chem. Soc.* **1960**, *82*, 4424–4426.

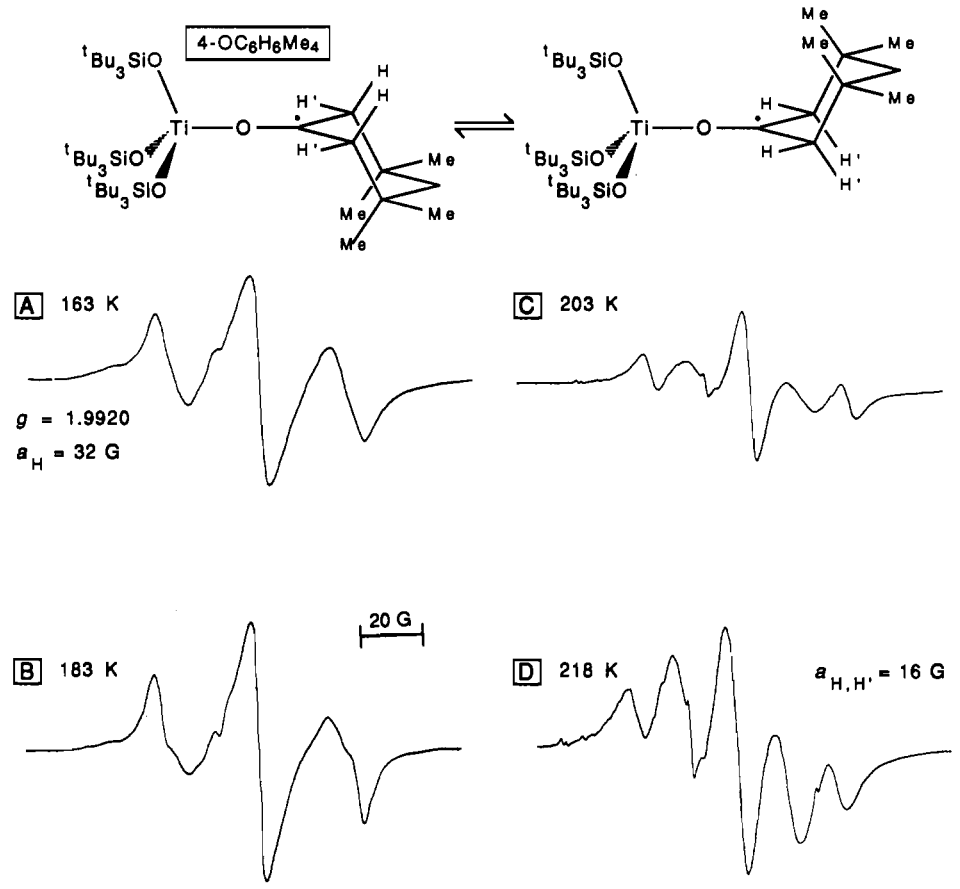

Figure 3. Variable-temperature EPR spectra (2-methylpentane) of $(silox)_3TiOC_6H_6Me_4$ (**4**–$OC_6H_6Me_4$). The fine structure on the broad features is due to a persistent, unidentified impurity that is still present after dissociation of 3,3,5,5-tetramethylcyclohexanone (>218 K) and reconstitution of the complex upon cooling.

= 19.0 G) with the aldehydic proton (Figure 2B). The doublet is anisotropic, and the high-field absorption manifests a small coupling due to the ^{t}Bu hydrogens of a = 0.4 G at low modulation (0.025 G). A small titanium (^{47,49}Ti) hyperfine coupling of a_{iso} = 3.0 G was also observed, as well as a 40.4-G coupling tentatively assigned to the 1.1% of 4–O^{13}CH^{t}Bu present. Degradation of 4–OCH^{t}Bu to uncharacterized products ultimately occurred as evidenced by disappearance of the EPR signals above 253 K.

Since the H-atom abstraction depicted in Scheme I is a bimolecular process, ketyls possessing β-hydrogens should be observable, provided appropriate steric shielding is applied. The ketyl derived from 3,3,5,5-tetramethylcyclohexanone and $(silox)_3Ti$ (**4**) (eq 9) displayed the temperature-dependent EPR spectra illus-

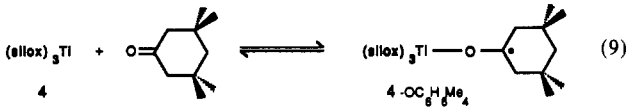

(9)

trated in Figure 3. At 218 K, a quintet arising from a_H = 16 G is centered at g = 1.9920 (spectrum D), but at 163 K, a 1:2:1 triplet is observed, with a_H = 32 G (spectrum A). Complete averaging of the β-hydrogens must occur somewhat higher than 218 K, since the quintet in spectrum D does not display the expected 1:4:6:4:1 intensity pattern. Unfortunately, at temperatures above 218 K, loss of the ketone broadened the spectral features[43] and prevented further interpretation, although this is probably not the mechanism of equilibration, since the 163–218 K spectra display the same total spread. Substantial degradation of the ketone did not occur, since the 163 K spectrum could be reconstituted. It is reasonable to view the dynamics in $(silox)_3Ti(OC_6H_6Me_4)$ (**4**–$OC_6H_6Me_4$) as an interconversion of two nonplanar six-membered rings, as previously observed for cyclohexyl radical[44–46] and 1-hydroxycyclohexan-1-yl.[46–48]

Acetophenone and $(silox)_3Ti$ (**4**) also formed an adduct, according to a complex absorption in the EPR spectrum at g = 2.002 for 4–OCMePh,[49] but rapid decomposition generated products that had overlapping spectral lines, thus preventing meaningful interpretation. Degradation of the acetophenone adduct was attributed to the H atom transfer chemistry described above. Since benzophenone would not be subject to this decomposition route, $(silox)_3Ti$ (**4**) was treated with a stoichiometric amount of $Ph_2C{=}O$ at −78 °C. In contrast to the previous substrates, when warmed to 23 °C the toluene solution turned deep red and rapidly faded to yellow. A yellow powder corresponding to a 1:1 benzophenone–**4** complex was isolated; temperature- and concentration-dependent ^{1}H and $^{13}C\{^1H\}$ NMR spectra were characteristic of an asymmetric dimer. Further analysis revealed a structure resulting from coupling of the para carbon of a phenyl group with the carbonyl carbon of another adduct (Scheme II), reminiscent of the coupling of trityl radicals.[50,51]

(43) (a) Hirota, N.; Weissman, S. I. *J. Am. Chem. Soc.* **1964**, *86*, 2537–2538. (b) Hirota, N.; Weissman, S. I. *Ibid.* **1964**, *86*, 2538–2545.

(44) (a) Ogawa, S.; Fessenden, R. W. *J. Chem. Phys.* **1964**, *41*, 994–998. (b) Bonazzola, L.; Leray, N.; Marx, R. *Chem. Phys. Lett.* **1974**, *24*, 88–90.

(45) For a general description of the EPR spectra of alkyl radicals, see: Fessenden, R. W.; Schuler, R. H. *J. Chem. Phys.* **1963**, *39*, 2147–2195.

(46) For conformational information of cyclohexyl radicals and 1-hydroxycyclohexan-1-yl, see: (a) Simamura, O. In *Topics in Stereochemistry*; Eliel, E. L., Allinger, N. L., Eds.; John Wiley & Sons: New York, 1969; Vol. 4, pp 1–37. (b) Gerson, F. *High Resolution E.S.R. Spectroscopy*; John Wiley and Sons: New York, 1970. (c) Fraenkel, G. K. *J. Phys. Chem.* **1967**, *71*, 139–171.

(47) Corvaja, C.; Giacometti, G.; Sartori, G. *J. Chem. Soc., Faraday Trans. 2* **1974**, *70*, 709–718.

(48) For comparison to 2-hydroxypropan-1-yl, see: Livingston, R.; Zeldes, H. *J. Chem. Phys.* **1966**, *44*, 1245–1259.

(49) For the EPR spectra of benzaldehyde and acetophenone radical anions, see: Steinberger, N.; Fraenkel, G. F. *J. Chem. Phys.* **1964**, *40*, 723–729.

Scheme II

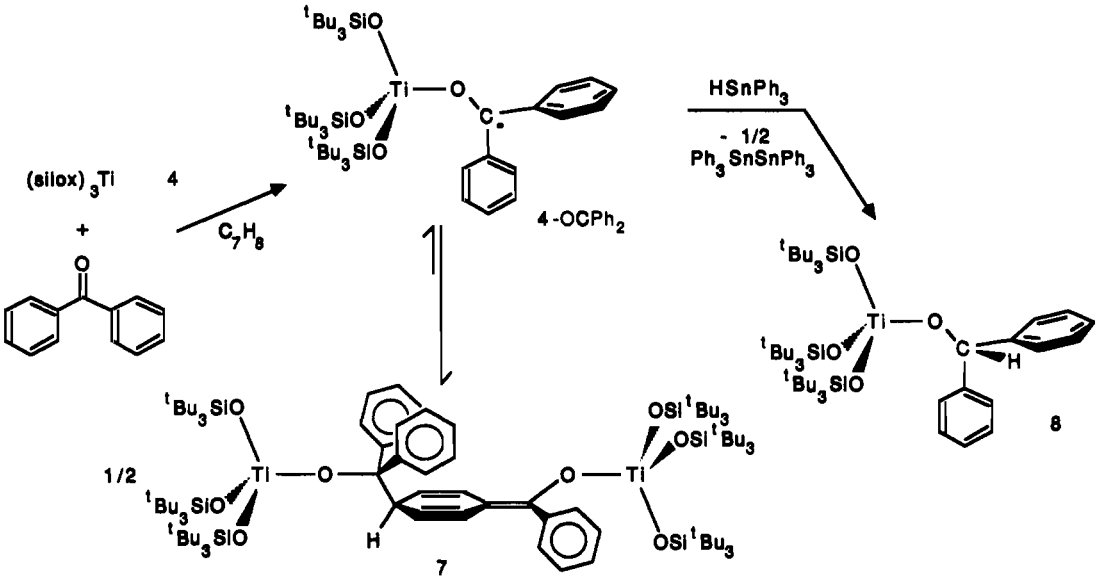

The dimer (silox)$_3$Ti—O(Ph)$_2$C=(H)C(CH)$_2$C(CH=CH)=C(Ph)O—Ti(silox)$_3$ (or [(silox)$_3$Ti(OCPh$_2$)]$_2$, **7**) logically arises from coupling of ketyl (silox)$_3$Ti(OCPh$_2$•) (**4**–OCPh$_2$). Confirmation of this pathway was achieved via spectroscopic and chemical means. As Scheme II illustrates, the addition of Ph$_3$SnH to solutions of **7** yielded (silox)$_3$TiOCPh$_2$H (**8**, 43%) and Ph$_3$SnSnPh$_3$, indicative of ketyl trapping by the hydrogen atom donor.[52] Furthermore, the reaction implicated an equilibrium between **7** and 2.0 equiv of ketyl **4**–OCPh$_2$. In support, ^{1}H NMR and EPR spectra taken of the same solution revealed the presence of both paramagnetic (**4**–OCPh$_2$) and diamagnetic (**7**) species.

Ketyl **4**–OCPh$_2$ gave a complicated 25 °C EPR signal containing >125 lines centered at g = 2.0005 (Figure 4A) that was diagnostic of a diaryl ketyl. For example, the EPR spectrum of Na(OCPh$_2$) is centered at g = 2.00 with a_H(ortho) = 2.6 G, a_H(meta) = 0.8 G, and a_H(para) = 3.4 G.[53] Attempts to simulate the spectrum of **4**–OCPh$_2$ were only partly successful. Hyperfine couplings of $a \sim$ 1–5 G (e.g., 4 $a_H \sim$ 1 G, 4 $a_H \sim$ 2.5–2.8 G, 2 $a_H \sim$ 5.3 G) were used to fit approximately two-thirds of the spectrum, and it became clear that very subtle changes (e.g., variations of 0.001–0.01 G) would be necessary to verify all of the lines. The complexity and number of lines implicate inequivalent phenyl rings, hindered ring rotation, or both.

Although no obvious ^{47,49}Ti satellites were apparent, it was plausible that they interfered with the interpretation and fitting of the spectrum. Use of benzophenone-d_{10} compressed the complex signal by a factor of γ_D/γ_H = 0.154.[37] The outer lines of the distinctive titanium hyperfine pattern should be visible if a_{Ti} were at least 2 G, but the EPR spectrum of the ketyl **4**–OCPh$_2$-d_{10} did not reveal titanium hyperfine coupling, although a carbonyl coupling of a_C = 27 G and residual ^{1}H coupling of ~5.2 G are observed (Figure 4B). It is possible that the difficulties encountered in fitting the central portion of the EPR spectrum result from interference due to a small titanium hyperfine coupling (e.g., a_{Ti} < 2 G).

Upon heating samples in the probe of the EPR spectrometer from −50 to +100 °C, the signal intensity increased and substantial changes in the spectrum were noted. At temperatures >100 °C, rapid decomposition occurred. Cooling the sample from 100 to 25 °C afforded a signal for **4**–OCPh$_2$ that was substantially less than the original intensity, indicative of some degradation. Furthermore, this EPR signal deviated from the initial 25 °C spectrum, suggesting that impurities were being introduced in the

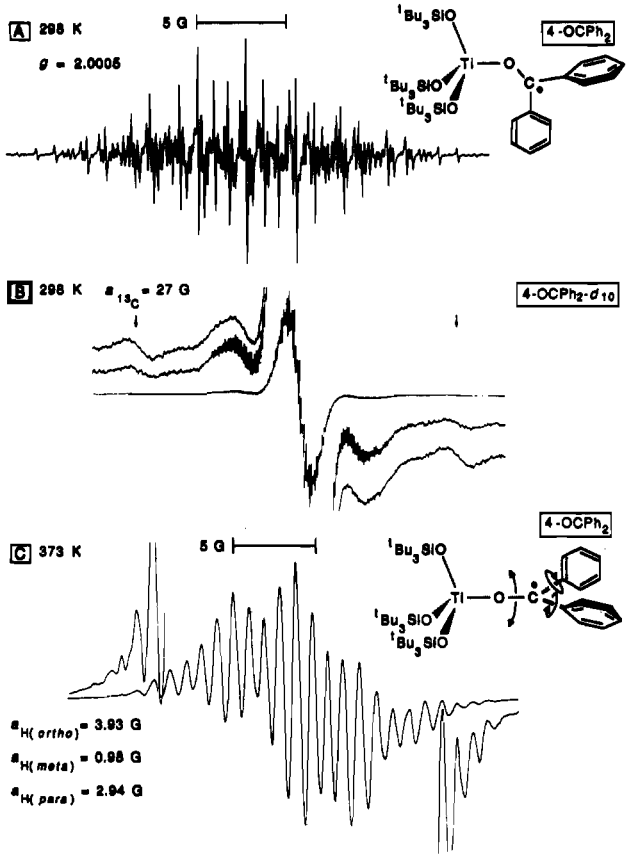

Figure 4. (A) EPR spectrum (toluene) of (silox)$_3$Ti(OCPh$_2$•) (**4**–OCPh$_2$) showing >125 lines indicative of inequivalent Ph rings, hindered ring rotation, or both. (B) Compressed EPR spectrum (toluene) of **4**–OCPh$_2$-d_{10} revealing a lack of notable Ti hyperfine lines (a_{Ti} < 2 G), a residual proton coupling, and a ^{13}C splitting. (C) EPR spectrum (toluene) of **4**–OCPh$_2$ at 100 °C, exhibiting 27 lines as ring equilibration is nearly complete.

(50) (a) Gomberg, M. *J. Am. Chem. Soc.* **1900**, *22*, 757–771. (b) Sholle, V. D.; Rozantsev, E. G. *Russ. Chem. Rev. (Engl. Trans.)* **1973**, *42*, 1011–1019.
(51) Neumann, W. P.; Uzick, W.; Zarkadis, A. K. *J. Am. Chem. Soc.* **1986**, *108*, 3762–3770.
(52) Tanner, D. D.; Diaz, J. E.; Potter, A. *J. Org. Chem.* **1985**, *50*, 2149–2150.
(53) The two equivalent Ph groups in Na$^+$[Ph$_2$C=O]$^-$ give rise to a 75-line pattern as described. Under some conditions (Na/THF, Na/dioxane), the EPR spectrum of benzophenone radical anion revealed more complicated hyperfine splitting patterns attributed to slow rotation of the phenyl rings. (a) Ayscough, P. B.; Wilson, R. *J. Chem. Soc.* **1963**, 5412–5417. (b) Dams, R.; Malinowski, M.; Westdorp, I.; Geise, H. Y. *J. Org. Chem.* **1982**, *47*, 248–259.

Scheme III

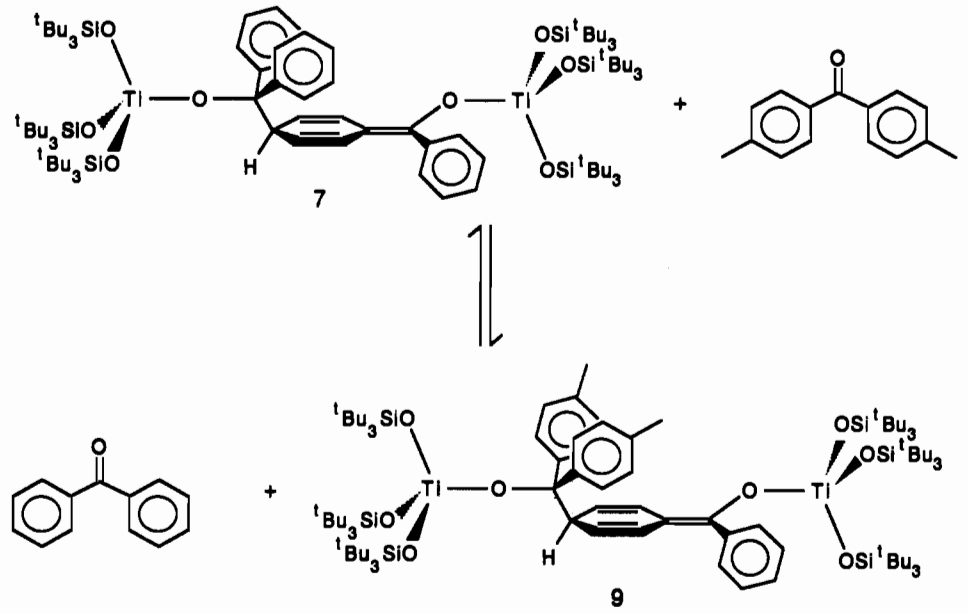

system. A qualitative interpretation of the fluxionality can be obtained from the 100 °C EPR spectrum (Figure 4C). The relative broad line widths (~0.5 G) of the 27-line pattern are indicative of a coalescence,[37-39,54] and the spectrum can be interpreted as approaching a quintet (a_H(ortho) = 3.93 G) of quintets (a_H(meta) = 0.98 G) of triplets (a_H(para) = 2.94 G). This assessment makes chemical sense if the phenyl groups of the ketyl are becoming equivalent while freely rotating. Furthermore, the values are consistent with the attempts at fitting the 25 °C EPR spectrum. If the ortho positions of the phenyl rings in the 25 °C static structure exhibited a_H(ortho) ~ 2.5 and 5.3 G, coalescence would lead to a a_H(ortho) of approximately 3.9 G.

An intense blue solution formed when (silox)$_3$Ti (**4**) was exposed to 4,4′-dimethylbenzophenone (eq 10), since blocking the para

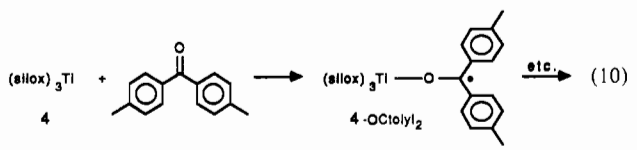

(10)

positions of diaryl ketones inhibits the coupling reaction. The 218 K EPR spectrum of (silox)$_3$Ti–OC(C_6H_4Me)$_2$• (**4**–OC(tolyl)$_2$) consisted of >66 lines centered at g = 2.0004.[55] Again the hyperfine couplings due to hydrogen ranged from ~1 to ~5 G, and the spectrum was not simulated. Upon warming, the solution gradually discolored, and its ^{1}H NMR spectrum revealed several products. H atom transfer reactions involving weaker benzylic C–H bonds are plausible degradation steps.

Evidence clearly suggests that carbon–carbon bond formation to generate dimer **7** is reversible, but the degree of benzophenone lability in ketyl **4**–OCPh$_2$ is unknown. When (silox)$_3$Ti—O-(Ph)$_2$C(H)C(CH)$_2$C(CH=CH)=C(Ph)O—Ti(silox)$_3$ (**7**) was exposed to 1.0 equiv of 4,4′-dimethylbenzophenone, a ^{1}H NMR spectrum of the mixture revealed the presence of benzophenone, a new set of resonances akin to and partly overlapping those of **7**, and new Me absorptions. Crossover to form an equilibrium mixture containing the mixed diaryl ketone dimer (silox)$_3$Ti—O(tolyl)$_2$C(H)C(CH)$_2$C(CH=CH)=C(Ph)O—Ti(silox)$_3$ (**9**, Scheme III) has occurred. The para positions of 4,4′-dimethylbenzophenone are capped, so dimerization must occur through the phenyl ring of the unsubstituted benzophenone. This must be considered tentative evidence for the *dissociative* loss of benzophenone from **4**–OCPh$_2$, since an associative displacement would also cause exchange. Nonetheless, given the reversibility of previously described ketyl complexes, **4**–OCPh$_2$ must be considered a labile species.

Since [(silox)$_3$Ti(OCPh$_2$)]$_2$ (**7**) and (silox)$_3$Ti(OCPh$_2$•) (**4**–OCPh$_2$) were observed in solution, it was possible to measure the equilibrium constant. Quantitative EPR measurements (spin-counting) should give the concentration of **4**–OCPh$_2$,[37-39] but practical considerations necessitated a swifter spectroscopic technique to quantitate the relative concentrations of **4**–OCPh$_2$ and **7**. Yellow solutions of **7** showed an absorption at 646 nm when heated in the sample chamber of a UV–vis spectrophotometer. The intensity of this absorption increased with heating and decreased when cooled, indicating the presence of **4**–OCPh$_2$.

The monomeric ditolyl ketyl (silox)$_3$Ti—OC(C_6H_4Me)$_2$• (**4**–OC(tolyl)$_2$), showed a similar absorption at 692 nm. To quantify the molar absorptivity for this band, samples were prepared in situ from (silox)$_3$Ti (**4**) and excess (2–5 equiv) 4,4′-dimethylbenzophenone. The UV–vis spectrum of **4**–OC(tolyl)$_2$ was measured within 1 min of ketyl formation, prior to significant decomposition, and an average molar absorptivity of 1800 M^{-1} cm^{-1} was obtained after several trials. Under conditions of excess 4,4′-dimethylbenzophenone, the half-life for decay of the intensity of the absorption, and therefore the decomposition of **4**–OC(tolyl)$_2$, was ~10 min.

Assuming the same molar absorptivity (ϵ = 1800 M^{-1} cm^{-1}) for the absorption pertaining to (silox)$_3$Ti(OCPh$_2$•) (**4**–OCPh$_2$), the equilibrium concentrations of **4**–OCPh$_2$ and dimer **7** were determined over a temperature range of 24 to 86 °C. From the temperature dependence of the equilibrium constant, the enthalpy and entropy associated with the reversible carbon–carbon bond formation was obtained through the van't Hoff equation. The equilibrium constant was defined as the dissociation of **7** into 2 equiv of **4**–OCHPh$_2$ (K_{eq} = [**4**–OCPh$_2$]^2/[**7**]; eq 11). Three trials

$$\underset{\mathbf{7}}{[(\text{silox})_3\text{Ti}(\text{OCPh}_2)]_2} \rightleftharpoons 2\underset{\mathbf{4}\text{–OCPh}_2}{(\text{silox})_3\text{Ti}(\text{OCPh}_2\text{•})} \qquad (11)$$

with nominal concentrations of **7** ranging from 4.4 × 10^{-4} to 1.1 × 10^{-3} M in hexanes were conducted, with linear plots of ln (K_{eq}) vs $1/T$ obtained for all concentrations. The concentration of **7** had little or no effect on the magnitude of ΔH or ΔS, and neither did changes in the solvent (hexane vs toluene) or the addition of a 10-fold excess of benzophenone. Thermodynamic parameters from the van't Hoff plots were ΔH_{diss} = 18 (1) kcal mol^{-1} and ΔS_{diss} = 33 (3) eu, while the equilibrium constant at 25 °C was K_{eq}(25 °C) = 7.5 × 10^{-7} M.

(54) Sullivan, P. D.; Bolton, J. R. *Adv. Magn. Reson.* **1970**, *4*, 39–85.
(55) For the EPR of 4,4′-dimethylbenzophenone, see: Kazakova, V. M.; Syrkin, Y. K.; Lipkind, G. M. *J. Struct. Chem. (Engl. Trans.)* **1963**, *4*, 841–842.

Table I. Ti XPS Data (eV) for Silox and Cp/Cp* Titanium Complexes[a,58]

	$(silox)_3TiCl$	$(silox)_2TiCl_2$	Cp_2TiCl_2	$Cp^*_2TiCl_2$
$Ti(2p_{1/2})$	465.00	464.40	463.35 (463.0)	(462.2)
$Ti(2p_{3/2})$	459.20	458.70	457.45 (456.9)	(456.1)

[a] All spectra internally referenced to carbon (284.60 eV). $Ti(2p_{3/2})$ shows a lower binding energy and is 2–3 times more intense than $Ti(2p_{1/2})$. Values in parentheses are from ref 57.

Discussion

Reduction of $(silox)_nMCl_m$. A principal factor in the chemistry of silox derivatives is the electrophilicity imparted to a metal center upon ligation by the bulky siloxides. While possessing a cone angle ($\angle \sim 125°$) approaching that of cyclopentadienyl ($\angle \sim 135°$),[29] silox donates far less electron density to a metal and is usually considered a $3e^-$ donor. In view of the purported hard character of the $^tBu_3SiO^-$,[28-33] it is somewhat surprising that low-valent-metal centers may be supported by this ligand. Unfortunately, quantification of the electronic properties the silox ligand is difficult to achieve.

X-ray Photoelectron Spectroscopy[56] has been utilized by Gassman[57] and Feher[58] to directly measure the relative electrophilicities of Cp_2TiCl_2 vs $Cp^*_2TiCl_2$ ($Cp^* = \eta^5$-C_5Me_5; M = Ti, Zr, Hf) derivatives. With accompanying electrochemical studies, Gassman et al. concluded that the substitution of two cyclopentadienyl ligands by two permethylcyclopentadienyl groups has an electronic effect approaching a one-electron reduction, since a 0.8 eV difference in binding energies (BE) was typically observed.[57] Table I lists more recent $Ti(2p_{1/2})$ and $Ti(2p_{3/2})$ binding energies for Cp_2TiCl_2, $Cp^*_2TiCl_2$, $(silox)_3TiCl$ (**1**), and $(silox)_2TiCl_2$.[36] Although both Cp_2TiCl_2 and $(silox)_2TiCl_2$ formally contain Ti(IV), the $Ti(2p_{3/2})$ binding energies show that the silox derivative is 1.25 eV more difficult to ionize. Substitution of chloride by another silox results in another increase of 0.50 eV in $Ti(2p_{3/2})$ binding energy. According to the XPS data, silox renders a metal center approximately 0.5 eV more electrophilic than either chloride or Cp, presumably due to the electronegativity of oxygen in combination with a diminished capacity for $O(p\pi) \rightarrow Ti(d\pi)$ donation. The latter may be partly due to $O(p\pi) \rightarrow Si(d\pi)$ interactions.

The XPS data do provide a rationale for the unexpected stability of low-valent silox derivatives. From the independent studies by Gassman and Feher, it can be inferred that a reduced titanium(III) siloxide (e.g., $(silox)_3Ti$ (**4**)) should have a BE similar to that of Cp_2TiCl_2. Provided the binding energies also reflect the thermodynamic stability of a compound, it is clear that silox is compatible with a reduced metal center, one that remains very electrophilic. The combination of potent reduction potential and electrophilicity has been previously espoused as the critical properties that enable $(silox)_3Ta$ to reduce and cleave carbon monoxide.[30]

The inability to prepare and isolate $(silox)_3Zr$ is disappointing, but not unexpected given the paucity of Zr(III) compounds devoid of Zr–Zr bonds.[59] It is also certain that $(silox)_3Zr$ would be extremely reactive, because $(silox)_3Ti$ (**4**) has been shown to react with ethers.[40] Since the electrochemical measurements indicated that $(silox)_3ZrX$ (X = Cl (**2**), I (**3**)) was reducible, it is likely that $(silox)_3Zr$, if generated, was simply too reactive to permit isolation.

Physical Studies of $(silox)_3Ti$ (4). The solution and powder EPR spectra of $(silox)_3Ti$ (**4**) are characteristic of an axially symmetric d^1 complex, with $g_{iso} = 1.9554$ deviating from the free electron value due to spin–orbit coupling. The large a_{iso} of 155 MHz ($\sim$56.7 G) is consistent with an electron occupying a $3d_{z^2}$ orbital, since extensive mixing with the 4s orbital is predicted in D_{3h} or lower symmetry. Using Morton's atomic parameters[60] derived from Hartree–Fock–Slater atomic orbitals of Herman and Skillman,[61] the composition of the occupied orbital can be approximated. From the tabulated Ti data, the a_{iso} of 155 MHz leads to $\sim$20% 4s character, and the anisotropic parameter (i.e., $^1/_3(a_\parallel - a_\perp)$) predicts $\sim$30–40% $3d_{z^2}$ character for the molecular orbital. The large error in the latter is due to the ambiguity regarding the magnitude of $a_\perp$. By difference, the data also predicts that this orbital should have 40–50% ligand character, a result somewhat suspect in view of the electronegativity differences between titanium and oxygen. Extended Hückel molecular orbital calculations on **4** corroborated the 4s number ($\sim$19%), but suggested that the orbital is almost purely metal-localized, since the $3d_{z^2}$ composition was $\sim$79%.[62] Prudence dictates that these estimations be treated as extremes, given the difficulties inherent to both types of approximations.

Table II. Comparative UV–Vis and EPR Spectral Analysis of X_3Ti Complexes (Values Estimated on the Basis of $\lambda = 106$ cm^{-1} in Parentheses)

param	$[(Me_3Si)_2N]_3Ti$[a]	$(Ar'O)_3Ti$[b]	$(silox)_3Ti$ (**4**)
$E(^2A_1' \rightarrow {}^2E')$, cm^{-1}	17400	17200	20000
ϵ M^{-1} cm^{-1}	122	75	350
$E(^2A_1' \rightarrow {}^2E'')$, cm^{-1}	4800		
ϵ, M^{-1} cm^{-1}	10		
$g_\perp$	1.869	1.926	1.9323
$g_\parallel$	1.993	1.998	1.9997
λ/Δ	0.0222	0.01272	0.01167
λ, cm^{-1}	107		
Δ, cm^{-1}	4800	(8420)	(9170)
D_t/D_s	0.01199	(0.1267)	(0.1082)
$E(a_1')$, cm^{-1}	−8880	(−10250)	−11670
$E(e'')$, cm^{-1}	−4080	(−1830)	(−2500)
$E(e')$, cm^{-1}	8520	(6950)	(8330)
CFSE, cm^{-1}	8880	(10250)	(11670)

[a] The data for $[(Me_3Si)_2N]_3Ti$ are from ref 64. [b] The data for $(Ar'O)_3Ti$ (Ar'O = 2,6-di-*tert*-butylphenoxide) are from ref 65.

Trigonal early-transition-metal complexes containing sterically demanding ligands have previously undergone spectral analysis. Bradley's bright blue $[(Me_3Si)_2N]_3Ti$[63,64] and Rothwell's $(Ar'O)_3Ti$ (Ar'O = 2,6-di-*tert*-butylphenoxide)[65] compounds provide a ready comparison to $(silox)_3Ti$ (**4**), although the hyperfine couplings of neither were analyzed nor were these species structurally verified via X-ray crystallography.

For $[(Me_3Si)_2N]_3Ti$, the $^2A' \rightarrow {}^2E''$ ($(d_{z^2})^1 \rightarrow (d_{xz},d_{yz})^1$) and $^2A' \rightarrow {}^2E'$ ($(d_{z^2})^2 \rightarrow (d_{x^2-y^2},d_{xy})^1$) transitions (Figure 5) were observed at 4800 and 17400 cm^{-1}, respectively.[64] In a D_{3h} crystal field, Δ is defined as the difference between the $^2A_1'$ and $^2E''$ states (4800 cm^{-1}). A crystal field splitting diagram was derived using Wood's conventions (eqs 12–14) for the d-orbital energies in a

$$E(a_1') = 2D_s + 6D_t \quad (12)$$

$$E(e'') = D_s - 4D_t \quad (13)$$

$$E(e') = -2D_s + D_t \quad (14)$$

trigonal field, and the data are tabulated in Table II.[66] A frozen

(56) Ghosh, P. K. *Introduction to Photoelectron Spectroscopy*; John Wiley and Sons: New York, 1983.
(57) Gassman, P. G.; Macomber, D. W.; Herschberger, J. W. *Organometallics* **1983**, *2*, 1470–1472.
(58) Feher, F.; Wells, S.; Hemminger, J. Unpublished results.
(59) (a) Cardin, D. J.; Lappert, M. F.; Raston, C. L.; Riley, P. I. In *Comprehensive Organometallic Chemistry*; Wilkinson, G., Stone, F. G. A., Abel, E. W., Eds.; Pergamon: New York, 1982; Vol. 3, pp 606–609. (b) Wielstra, Y.; Gambarotta, S.; Spek, A. L.; Smeets, W. J. J. *Organometallics* **1990**, *9*, 2142–2148. (c) Wielstra, Y.; Gambarotta, S.; Meetsma, A. *Ibid.* **1989**, *8*, 2948–2952. (d) For in situ Zr(III), see: Samuel, E. *Inorg. Chem.* **1983**, *22*, 2967–2970.
(60) Morton, J. E.; Preston, K. F. *J. Magn. Reson.* **1978**, *30*, 577–582.
(61) Herman, F.; Skillman, S. *Atomic Structure Calculations*; Prentice-Hall: Englewood Cliffs, NJ, 1963.
(62) Wheeler, R. A.; Zonnevylle, M. C.; Wolczanski, P. T. Unpublished results.
(63) Alyea, E. C.; Bradley, D. C.; Copperthwaite, R. G. *J. Chem. Soc., Dalton Trans.* **1972**, 1580–1584.
(64) (a) Alyea, E. C.; Bradley, D. C.; Copperthwaite, R. G.; Sales, K. D. *J. Chem. Soc., Dalton Trans.* **1973**, 185–191. (b) Bradley, D. C.; Copperthwaite, R. G.; Cotton, R. G.; Sales, K. D.; Gibson, J. F. *J. Chem. Soc., Dalton Trans.* **1973**, 191–200.
(65) Latesky, S. J.; Keddington, J.; McMullen, A. K.; Rothwell, I. P.; Huffman, J. C. *Inorg. Chem.* **1985**, *24*, 995–1001.
(66) (a) Wood, J. S. *Inorg. Chem.* **1968**, *7*, 852–859. (b) Fenton, N. D.; Gerloch, M. *J. Chem. Soc., Dalton Trans.* **1988**, 2201–1988.

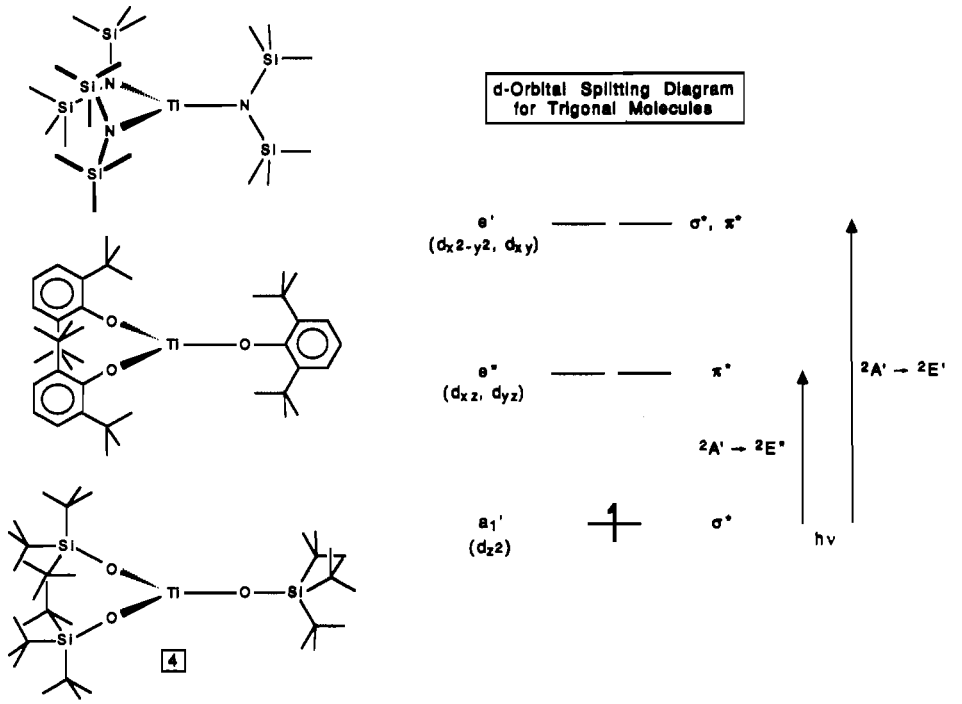

Figure 5. Probable geometries of $[(Me_3Si)_2N]_3Ti$, $(Ar'O)_3Ti$ (Ar'O = 2,6-di-*tert*-butylphenoxide) and $(silox)_3Ti$ (**4**), and a d orbital splitting diagram for trigonal molecules.

glass EPR spectrum of the tris(amide) ($g_\parallel = 1.993$, $g_\perp = 1.869$) enabled calculation of the spin–orbit coupling parameter, λ, according to eq 15,[37] where $g_e = 2.0023$, and the value of 107 cm^{-1}

$$g_\perp = g_e - 6\lambda/\Delta \qquad (15)$$

obtained represents ~69% of the free ion value for Ti^{III} (155 cm^{-1}).[67]

Figure 5 illustrates proposed structures of the trigonal compounds and a generic ligand field splitting diagram. The above analysis cannot be conducted for $(Ar'O)_3Ti$ and $(silox)_3Ti$ (**4**), since the electric-dipole-forbidden $^2A' \rightarrow {}^2E''$ transition was unobserved in both cases, despite exhaustive attempts to locate it. Some information can be gleaned from the λ/Δ parameter, which is determined directly from the powder EPR spectrum. The perturbation of $g_\perp$ from the free electron value is principally due to spin–orbit coupling arising via mixing of the first excited state, $^2E''$, with the ground state, $^2A_1'$.[37-39] The magnitude of the scalar spin–orbit coupling parameter, λ, is directly proportional to the perturbation, while the magnitude of Δ is inversely related, since the mixing will decline as the energy difference between $^2A_1'$ and $^2E''$ increases.

Table II shows that λ/Δ for $[(Me_3Si)_2N]_3Ti$ is nearly twice that of $(Ar'O)_3Ti$ and $(silox)_3Ti$ (**4**). A larger λ and/or a smaller Δ attributed to the tris(amide) vs the aryl oxide and siloxide complexes provides the rationale. The parameter λ is proportional to Z_{eff}/r^3, where r reflects the radial extent of the appropriate orbitals. Both of these factors are relatively insensitive to the nature of the ligand. For example, λ for atomic Ti^0 is 70 cm^{-1} compared with 155 cm^{-1} for a Ti^{3+} ion, a dramatic change in Z_{eff}.[67] In actuality, a slight increase in Z_{eff} might be expected for $(Ar'O)_3Ti$ or **4** vs $[(Me_3Si)_2N]_3Ti$ since electronegativity arguments suggest that the amide should form more covalent bonds. Regardless, Z_{eff} should be essentially equivalent for the three ligands. It is also unlikely that substantive changes in r result from the ligand differences, although in this instance the trend is at least correct. The plane of the $(Me_3Si)_2N$ ligand is presumably perpendicular to the trigonal plane, thus the nitrogen p orbitals will not interact with d_{xz} and d_{yz} (in reality the symmetry is probably somewhat lower (D_3),[68] resulting in a small interaction). The aryl oxide[65,69] and siloxide ligands have p orbitals with the appropriate symmetry to mix with the e'' set; thus, the d_{xz} and d_{yz} orbitals are not pure d and are expected to be radially somewhat more disperse. In summary, given these arguments and Bradley's observation that λ for Ti^{3+} declined only 31% for no ligands (free ion) in comparison to $[(Me_3Si)_2N]_3Ti$, the greater quenching of spin–orbit coupling for the oxygen-based ligands originates from a larger Δ.

In Table II, λ was assumed to be ~107 cm^{-1} for each complex, thereby permitting the calculation of Δ, $E(a_1')$, $E(e'')$, and $E(e')$ for $(Ar'O)_3Ti$ and $(silox)_3Ti$ (**4**). Silox must be considered slightly stronger or equivalent to the other ligands in view of the energies pertaining to the $^2A' \rightarrow {}^2E'$ transition and CFSE. A major difference between the amide and oxygen-based ligands arises from the energies of the e'' orbital set, which is much higher in the latter complexes due to the large difference in Δ. Although an amide is expected to be a slightly better π-donor than an alkoxide or siloxide, the aforementioned geometric constraints effectively restrict the π-donation of the bulky $(Me_3Si)_2N$ to orbitals in the xy plane. For $(Me_3Si)_2N$, e'' is essentially a nonbonding orbital, whereas it is decidely π* for the Ar'O and silox coordination spheres. The data, particularly the CFSE's, manifest the electronic similarities of the Ar'O and silox ligands. Parallels in the reactivity patterns and structures of early transition metal Ar'O[70,71] and

(67) Values taken from: (a) Figgis, B. N. *Introduction to Ligand Fields*; Interscience: New York, 1966. See also: (b) Weltner, W. *Magnetic Atoms and Molecules*; Van Norstrand Rheinhold: New York, 1983. (c) Weissbluth, M. *Atoms and Molecules*; Academic: New York, 1978.

(68) (a) For the D_3 structure of $[(Me_3Si)_2N]_3Fe$, see: Hursthouse, B.; Rodesiler, P. F. *J. Chem. Soc., Dalton Trans.* **1972**, 2100–2102. (b) For a similar structure of $[(Me_3Si)_2N]_3Sc$, see: Ghotra, J. S.; Hursthouse, B.; Welch, A. J. *J. Chem. Soc., Chem. Comm.* **1973**, 669–670.

(69) For the structure of $(Ar''O)_3Sc$ (Ar''O = 2,6-di-*tert*-butyl-4-methylphenoxide), see: Hitchcock, P. B.; Lappert, M. F.; Singh, A. *J. Chem. Soc., Chem. Commun.* **1983**, 1499–1501.

(70) (a) Ankianiec, B. C.; Fanwick, P. E.; Rothwell, I. P. *J. Am. Chem. Soc.* **1991**, *113*, 4710–4712. (b) Steffey, B. D.; Rothwell, I. P. *J. Chem. Soc., Chem. Commun.* **1990**, 213–215. (c) Hill, J. E.; Fanwick, P. E.; Rothwell, I. P. *Organometallics* **1991**, *10*, 15–16. (d) Hill, J. E.; Profilet, R. D.; Fanwick, P. E.; Rothwell, I. P. *Angew. Chem.* **1990**, *102*, 713–715. (e) Hill, J. E.; Nash, J. M.; Fanwick, P. E.; Rothwell, I. P. *Polyhedron* **1990**, *9*, 617–619. (f) Rothwell, I. P. *Acc. Chem. Res.* **1988**, *21*, 153–159 and references therein.

(71) (a) Bruck, M. A.; Copenhaver, A. S.; Wigley, D. E. *J. Am. Chem. Soc.* **1987**, *109*, 6525–6527. (b) Arney, D. J.; Wexler, P. A.; Wigley, D. E. *Organometallics* **1990**, *9*, 1282–1289. (c) Strickler, J. R.; Bruck, M. A.; Wigley, D. E. *J. Am. Chem. Soc.* **1990**, *112*, 2814–2816 and references therein.

Table III. EPR Data of Ketyl Complexes, $(silox)_3Ti(OCRR'^{\bullet})$ (**4**–OCRR'), and First Reduction Potentials of Selected O=CRR' Compounds

4–OCRR'/O=CRR'	g	a_{Ti}, G	a_H, G (assgnt)	a_C, G	T, K	$E_{1/2}$ vs SCE,[a] V
4–OC^tBu_2	1.9985	4	...	26	213	
4–OCH^tBu	2.0001	3	19 (*CH*) 0.4 (^{t}Bu)	40.4	203	
MeCHO	...	...	...	...	...	−2.03 (EtOH)
4–$OC_6H_6Me_4$	1.9920	...	16 $(C_\beta H_2)_2$[b] 32 $(C_\beta HH)_2$[b]	...	218 163	
c-$C_6H_{10}O$	...	...	...	...	...	−2.40 (EtOH)
4–OCMePh	2.002	...	complex	...	...	
PhCOMe	...	...	...	...	...	−1.60 (^{i}PrOH)[c]
4–$OCPh_2/OCPh_2$	2.0005	...	complex[b] 3.93 (ortho), 0.98 (meta) 2.94 (para)	...	298 373	−1.33 (^{i}PrOH)[d]
4–$OCPh_2$-d_{10}	2.0006	<2	complex[b]	27	298	
4–$OC(p\text{-tolyl})_2$	2.0004	...	complex[b]	...	218	

[a] Data from ref 72. [b] See text for explanation. [c] ECE; second reduction at −2.32 V. [d] ECE; second reduction at −2.69 V (DMF).

silox[29–33] derivatives also exist.

Ketyl Derivatives of $(silox)_3Ti$ (4). In general, the ligands of pseudotetrahedral adducts $(silox)_3TiL$ (**4**–L, L = DME, CNMe, CN^{t}Bu, NC^{t}Bu, PMe_3, NH_3) are weakly bound for reasons that have previously been expounded upon for related $(silox)_3TaL$ species.[32] In contrast the ketyl derivatives, **4**–L, did not display EPR spectra, even at 77 K. This behavior is predicted for d^1 C_{3v} complexes where occupation of the e″ orbitals (d_{xz}, d_{yz}) with one electron results in substantial spin–orbit interaction as evidenced by relaxation broadening.[38] For the cylindrically symmetric L above, a minor perturbation of the e″ set arises from a Jahn–Teller distortion, but the two resulting orbitals remain energetically similar and readily couple. Since the relaxation time is inversely proportional to temperature, further cooling of **4**–L might have allowed the observation of EPR signals.

Table III summarizes the EPR data of ketyl derivatives $(silox)_3Ti(OCRR'^{\bullet})$ (**4**–OCRR'), and reduction potentials of pertinent organic carbonyls. The ketyls possess C_s or lower symmetry rather than C_{3v}, since significant splitting of the low-lying d_{xz} and d_{yz} orbitals is necessary to minimize spin–orbit coupling and permit EPR observation in the 200–300 K regime. A truncated molecular orbital diagram depicting the crucial ketyl bonding orbitals is illustrated in Figure 6. The σ-bonding occurs via donation of an oxygen lone pair into an acceptor orbital (mostly d_{z^2}) of the pyramidal $(silox)_3Ti$ moiety, and the symmetry of the second "lone pair" enables it to π-bond with the d_{xz} of titanium, thereby generating the metal localized π^*-LUMO ("d_{xz}"). The C=O π^* orbital of the ketone/aldehyde interacts with d_{yz} to stabilize the latter, which is half-occupied (HOMO or SOMO). An added complication is the slight interaction of the C=O π-bonding orbital with d_{yz}. These three orbitals mix to generate a "d_{yz}" SOMO that has substantial Ti and carbon, but minimal oxygen character. The energy gap (ΔE) between molecular orbitals "d_{xz}" and "d_{yz}", which is critical in disengaging the aforementioned EPR relaxation broadening mechanism, thus depends on two factors: (1) the strength of $O(p\pi) \rightarrow Ti(d\pi)$ bonding, and (2) the magnitude of the $Ti(d\pi) \rightarrow C{=}O(\pi^*)$ interaction. From a valence-bond standpoint, a strong titanium–oxygen interaction implies that the ketyl resonance from (i.e., $(silox)_3Ti^{IV}$—O—CRR'$^{\bullet}$) predominates over a Ti(III) adduct form (i.e., $(silox)_3Ti^{III}$—O=CRR').

The g values attributed to the ketyls range from 1.9920 for **4**–$OC_6H_6Me_4$ to 2.002 for **4**–OCMePh and appear to reflect the degree of carbon character in the SOMO. Sterically bulky ketones that reversible bind to $(silox)_3Ti$ (**4**), such as $^tBu_2CO$ and 3,3,5,5-tetramethylcyclohexanone, exhibit lower g values as their respective ketyls, implicating increased spin–orbit interactions due to a smaller ΔE (Figure 6). Smaller (e.g., ^{t}BuCHO) or flatter (e.g., PhCOMe, Ph_2CO) carbonyls that can more easily access the titanium center display values nearer that of a free electron, similar to organic radicals. As the bonding changes from a purely dative interaction to the covalent titanium–oxygen single bond

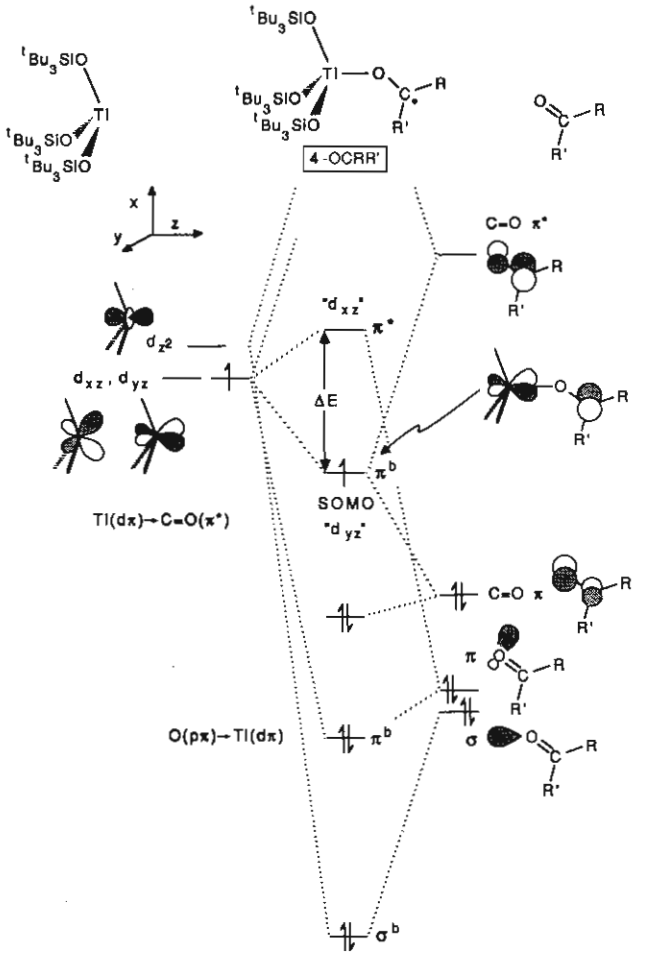

Figure 6. Molecular orbital diagram of a generic ketyl, **4**–OCRR', showing the critical orbital interactions.

of the ketyl structure, the Ti–O distance may contract by as much as 0.3–0.4 Å,[21,22] a significant difference.

Although the π-basicity of the RR'C=O substrates is difficult to assess, their reduction potentials are indicative of the C=O π^* energies and should crudely predict the relative ketyl SOMO energies. As Table III indicates, aliphatic ketones and aldehydes, represented by acetaldehyde and cyclohexanone, are more difficult to reduce than aromatic RR'C=O compounds. In accord with this reasoning, **4**–OC^tBu_2 and **4**–$OC_6H_6Me_4$ possess low g values, but unfortunately steric factors are also critical in both cases. Pivaldehyde binds to $(silox)_3Ti$ (**4**) quite strongly, given the g of 2.0001 and the sharp hyperfine lines (i.e., ΔE is large), contradicting the prediction based on reduction potential; however, aliphatic substrates should be stronger π-bases, and thus this data may indicate strong $O(p\pi) \rightarrow Ti(d\pi)$ bonding. As depicted in

(72) Meites, L.; Zuman, P., Eds. *The CRC Handbook Series in Organic Electrochemistry*; CRC Press: Cleveland, OH, 1977.

Figure 2B, steric problems may be minimized for 4–OCH^{t}Bu, since the bulky ^{t}Bu group can fit in the pocket of the silox groups while the C–H bond is directed toward them. Note that the reduction potentials of RR′C=O cannot be used to quantitatively rationalize the transfer of an electron from **4**, because ketyl formation is an inner-sphere process.

The "d_{yz}" SOMO is predicted to have little of the s character necessary to exhibit hyperfine titanium lines; thus, the lack of significant titanium hyperfine splittings in the ketyl complexes is expected. In comparison to benzaldehyde radical anion, which exhibits a 8.5-G splitting due to the aldehydic proton,[49] the 19-G hyperfine coupling displayed by 4–OCH^{t}Bu is quite substantial. Typical conditions to produce radical anions of aldehydes (e.g., Na^0 or K^0) result in the formation of RCO$^-$ and loss of hydrogen, so few examples of coupling to aldehydic protons exist. Presumably, similar decomposition pathways are responsible for the degradation of 4–OCH^{t}Bu above 253 K. Strong binding of pivaldehyde is also implicated by the large 40.4-G ^{13}C hyperfine coupling in 4–OCH^{t}Bu, especially when compared to the 26-G ^{13}C splitting of the more weakly bound ^{t}Bu$_2$CO complex, 4–OC^{t}Bu$_2$. Somewhat surprisingly, the benzophenone derivative 4–OCPh$_2$ displays a ^{13}C hyperfine coupling of only 27 G, perhaps as a consequence of the distribution of electron density into the π-system of the phenyl rings.

Steric factors also influence the conformation and dynamics of the ketyl ligand. It is plausible that one Ph group of 4–OCPh$_2$ is locked between two silox ligands (Figure 4), whereas the second is relatively central with respect to the surrounding ^{t}Bu groups, resulting in the inequivalent phenyls observed by EPR spectroscopy. When the sample is heated to 398 K, equilibration and free rotation of the phenyls are occurring on approximately the EPR time scale.

The substantial line widths ($\geq$5 G) of the spectra pertaining to (silox)$_3$Ti(OC$_6$H$_6$Me$_4$) (4–OC$_6$H$_6$Me$_4$) are attributed to spin–orbit relaxation broadening manifested by the g of 1.9920, as previously addressed. Additional broadening in spectra taken at >218 K is credited to ketone loss. As seen in Figure 3, 4–OC$_6$H$_6$Me$_4$ exhibits an alternating line-width effect[54] in its variable-temperature EPR spectra, which is expected for interchanging nonplanar structures. A plausible rationale would involve equilibrating chair $\rightarrow$ chair, or twist-boat $\rightarrow$ twist-boat conformations that interconvert different sets of C$_\beta$-hydrogens. Chair $\rightarrow$ chair changes apparently account for the dynamics in cyclohexyl radical,[44-46] and the C$_\beta$ hydrogen interchange in 1-hydroxycyclohexan-1-yl was rationalized as a twist-boat $\rightarrow$ twist-boat interconversion,[47] albeit with some uncertainty due to the likely possibility of nonplanar radical centers in both species.[46,73] The dynamic event exhibited by 4–OC$_6$H$_6$Me$_4$ occurs at lower temperatures, consistent with the potential outside steric influence of the tris(silox) coordination sphere and lower barriers associated with the 3,3,5,5-Me$_4$ substitution of the ketone. Ketyl structures that would cause C2 and C6 to be inequivalent do not appear to be relevant in view of the significant bulk of the ketone methyl groups and the similarity in dynamics to the organic systems.

Since hyperconjugation with the C$_\alpha$ p_z orbital is the primary coupling mechanism for β-hydrogens,[39] the magnitude of the C$_\beta$–proton hyperfine interaction is dependent on the angle (θ) between the p_z orbital of C$_\alpha$ and the C$_\alpha$–C$_\beta$–H plane. β-Hydrogens positioned axially are nearly parallel to p_z, while those in equatorial sites are virtually perpendicular to and are in the nodal plane of p_z; hence, coupling to the former should be substantially larger. The triplet at 163 K (A) displays only a large coupling of a_H = 32 G, while the other β-coupling is unresolved, but less than 5 G. The quintet at 218 K (D) reflects the equivalence of two types of β-hydrogens as the interconversion becomes fast on the EPR time scale, and $a_{obs} = 1/2(a_H + a_{H'}) = 16$ G, implying that the second $a_{H'} \sim 0$ G.

In the related 1-hydroxycyclohexan-1-yl radical, the β-axial coupling is 35.5 G, while the β-equatorial coupling is 10.3 G.[47] The data was treated using a modified McConnell equation,[39,74] $a_\beta = (B\rho_C)\cos^2\theta$, where B is a proportionality constant and ρ_C is the p_z or π-spin density on C$_\alpha$, neglecting an isotropic correction. Using an empirically generated $B\rho_C$ of 39.3 G, θ(H) = 18° and θ(H′) = 59°, values that are considered more consistent with a twist-boat (optimally θ(H) = 0°; θ(H′) = 60°) than a chair (optimally $\theta(H_{ax}) = 30°$; $\theta(H'_{eq}) = 90°$).[47] In this instance, $B\rho_C$ may be eliminated from the data treatment by noting that the β-hydrogens are constrained to be 120° apart. Combining $a_H = (B\rho_C)\cos^2\theta = 35.5$ G and $a_{H'} = (B\rho_C)\cos^2(60 - \theta) = 10.3$ and solving $a_H/a_{H'} = \cos^2\theta/\cos^2(\theta + 120°)$ yields angles of $\sim$3 and $\sim$57°, again more consistent with the twist-boat configuration. Although the ambiguity in $a_{H'}$ prevents the latter treatment of 4–OC$_6$H$_6$Me$_4$, the same $B\rho_C$ of 39.3 G for 4–OC$_6$H$_6$Me$_4$ results in values of 25° and 69° ($a_{H'} \sim 5$ G) to 90° (0 G). The uncertainty in $a_{H'}$ and difficulties in accurately evaluating $\cos^2\theta/\cos^2(\theta + 120°)$ hamper treatment of this ketyl, yet a *slight* preference for the chair $\rightarrow$ chair interconversion is evident. A stereochemical assessment of the related 3,3,5,5-tetramethylcyclohexanone clearly favors a chair configuration.[75] Given recent theoretical[73] and stereochemical studies, it is difficult to accept a twist-boat ground state for any of the above species.

Regardless of the actual ground-state conformation, the fact that 1-hydroxycyclohexan-1-yl and 4–OC$_6$H$_6$Me$_4$ can be at all compared via the McConnell relationship is an important verification of the ketyl formulation. It is unlikely that the proportionality constant B would vary significantly from the cyclohexyl radical ($B \sim 41$ G) and 1-hydroxycyclohexan-1-yl systems to the ketyl, 4–OC$_6$H$_6$Me$_4$. Therefore, the π-spin densities on C$_\alpha$ must be similar in all of these radicals, and 4–OC$_6$H$_6$Me$_4$ is appropriately depicted as a ketyl. In view of recent calculations,[73] it is conceivable that a dramatic pyramidalization at the C$_\alpha$ in 4–OC$_6$H$_6$Me$_4$ could skew the data, resulting in a misinterpretation, but the observation of significant spin density on C$_\alpha$ cannot be refuted.[76]

Ketyl Coupling. To a crude approximation, the formation of a ketyl complex can occur provided the Ti—O bond is stronger than the ketone/aldehyde C=O π-bond ($\sim$70 kcal/mol).[77] Thermochemical data on Ti(O^{t}Bu)$_4$ (D(Ti–O)$_{av}$ = 104 kcal/mol) and Ti(O^{i}Pr)$_4$ (106 kcal/mol)[78] indicate that Ti–O bond strengths are considerably greater, although it is likely that the first bond disruption enthalpy for a Ti(OR)$_4$ species is <100 kcal/mol. The oxophilic nature of titanium undoubtedly encourages strong π-donation from an OR ligand, providing the driving force for ketyl formation and pinacol synthesis, provided the latter dimerization is permitted by sterics. Changes in silox bonding due to the distortion from trigonal to pseudotetrahedral geometry should not be applicable, since the expected small increase in Ti^{IV}–O vs Ti^{III}–O bond strengths will be counteracted by increasing steric demands. In concert with the electropositive character of the Ti(III) center, (silox)$_3$Ti (**4**) is a potent reductant, a component that is inclusive in the bond strength criteria above. The direct observation of these Ti(III) ketyls and their subsequent chemistry support the current mechanistic hypotheses regarding pinacol coupling.

The steric influence of the tris(silox) coordination sphere is a major factor in the equilibria governing ketyl formation and is also manifested by the coupling of two benzophenones ketyls to

(73) Lloyd, B. V.; Causey, J. G.; Momany, F. A. *J. Am. Chem. Soc.* **1980**, *102*, 2260–2263.

(74) McConnell, H. M.; Chestnut, D. B. *J. Chem. Phys.* **1958**, *28*, 107–117.

(75) Kellie, G. M.; Riddell, F. G. In *Topics in Stereochemistry*; Eliel, E. L., Allinger, N. L., Eds.; John Wiley & Sons: New York, 1974; Vol. 8, pp 225–269.

(76) For an interesting comparison, note that radical anions of Fischer carbene complexes possess substantial spin density on the carbene carbon. See: (a) Krusic, P. J.; Klabunde, U.; Casey, C. P.; Block, T. F. *J. Am. Chem. Soc.* **1976**, *98*, 2015–2018. (b) Casey, C. P.; Albin, L. D.; Saeman, M. C.; Evans, D. H. *J. Organomet. Chem.* **1978**, *155*, C37–C40.

(77) Calculated from ΔH_f's and relevant thermochemical data in: (a) Carpenter, B. K. *Determination of Organic Reaction Mechanisms*; Wiley-Interscience: New York, 1984. (b) Benson, S. W. *Thermochemical Kinetics*; John Wiley and Sons: New York, 1968.

(78) Tel'noi, V. I.; Rabinovich, I. B. *Russ. Chem. Rev. (Engl. Transl.)* **1977**, *46*, 689–705.

form $[(silox)_3Ti(OCPh_2)]_2$ (**7**). Apparently, pinacol coupling of the C_α carbonyl carbons to produce a $-OCPh_2CPh_2O-$ bridge is sterically prohibited, leading to the para phenyl/carbonyl carbon coupling (C_α–C_{para}) analogous to the reversible dimerization of triphenylmethyl radical. Some evidence for reversible coupling of benzophenone by $CpTiCl_2$ has been presented,[14] although a ν(C–O) in the IR spectrum provided the sole evidence for a reduced carbon–oxygen bond order; the connectivity of the purported coupled product was not determined.

Another pinacol/ketyl equilibrium has been measured between silylated pinacols and silylated ketyls.[79] Photolysis of $(Me_3Si)_2Hg$ in the presence of benzophenone provided an equilibrium mixture of $Me_3SiOCPh_2^\bullet$ and $Me_3SiO(Ph)_2CC(Ph)_2OSiMe_3$. The EPR spectrum of the ketyl is similar to that of benzophenone radical anion; the dimer-to-monomer dissociation enthalpy was 31 kcal/mol.[80] Substituents on the aryl ring, particularly in the ortho position, have a profound effect on the dissociation enthalpy. The dimer of $Me_3SiOC(o\text{-tolyl})_2$, readily dissociates ($\Delta H_{diss}$ = 22 kcal/mol), while $Me_3SiOC(2,6\text{-xylyl})_2$, does not dimerize at all.

The dissociation enthalpies for trityl dimer (12 kcal/mol),[50] $[(silox)_3Ti(OCPh_2)]_2$ (**7**) (18 kcal/mol), and $Me_3SiO(Ph)_2CC(Ph)_2OSiMe_3$ (31 kcal/mol)[80] are quite different. The phenyl π-systems of **4**–$OCPh_2$, $Ph_3C^\bullet$, and $Me_3SiOCPh_2^\bullet$ are not wholly coplanar with the half-occupied C_α p_z orbital; thus, the resonance stabilization of the respective radicals is reduced, encouraging dimerization. The much smaller ΔH_{diss} for **7** and $[Ph_3C]_2$ may be attributed to the disruption of the aromaticity in one phenyl ring, a factor not relevant to the silylated example.

Trityl dimer is often used as a source of reactive $Ph_3C^\bullet$, a hydrogen atom abstractor. The C_α–C_{para}-coupled species dissociates to $Ph_3C^\bullet$ with an equilibrium constant of $K_{eq} = 2.2 \times 10^{-4}$ (22 °C). In dilute solutions (10^{-3} M) at 22 °C, 21% of the trityl dimer has dissociated to $Ph_3C^\bullet$, while ~1.3% of **7** has dissociated to ketyl **4**–$OCPh_2^\bullet$ under comparable conditions ($K_{eq} = 7.5 \times 10^{-7}$; at 70 °C, $K_{eq} = 5.6 \times 10^{-5}$, 11% dissociation).

As Scheme II depicts, the dissociation of **7** to 2 equiv of **4**–$OCPh_2^\bullet$ occurred rapidly, as detected by the production of $(silox)_3TiOCPh_2H$ (**8**) in the presence of Ph_3SnH. Although it is convenient to view the diphenylmethoxide product (**8**) as the direct product of hydrogen atom transfer to **4**–$OCPh_2^\bullet$, the possibility of a direct reduction of free benzophenone by Ph_3SnH cannot be completely ruled out.[52] Scheme III suggests that dissociation of $Ph_2C{=}O$ from **7**, followed by Ph_3SnH reduction to $Ph_2HCO^\bullet$, and competitive recapture of the latter by $(silox)_3Ti$ (**4**) instead of $Ph_3Sn^\bullet$ is a plausible alternative. Regardless, both possibilities require the cleavage of the C_α–C_{para} bond. In view of the purported disproportionations of $(silox)_3Ti(OCMeR^\bullet)$ (**4**–OCMeR, R = H, Me) that clearly involve hydrogen atom transfer (Scheme I), $H^\bullet$ transfer from Ph_3SnH to **4**–$OCPh_2^\bullet$ must be considered the favored pathway. Interestingly, a comparable chemistry of silylated aryl methyl ketyls has been observed. Generation of $Me_3SiOC(Me)Ph^\bullet$ resulted in either C_α–C_α dimerization, or disproportionation to $Me_3SiOC(Me)PhH$ and $Me_3SiOC(Ph){=}CH_2$ via H atom abstraction reactions, depending on the aromatic ring substituents.[79,80] Further redox studies of $(silox)_3Ti$ (**4**) and related complexes are ongoing.

Experimental Section

General Considerations. All manipulations were performed using standard glovebox or high-vacuum-line techniques. Ethereal and hydrocarbon solvents were distilled under nitrogen from purple Na/benzophenone ketyl and vacuum transferred from the same prior to use. Small amounts of tetraglyme (2–5 mL/L of solvent) were added to hydrocarbons to solubilize the ketyl. NMR solvents were dried over activated sieves, vacuum distilled, and stored in the glovebox or vacuum distilled from purple Na/benzophenone ketyl (C_6D_6 and THF-d_8). Zirconium tetrachloride was sublimed (Alfa, ~180°, 10^{-4} Torr) before use. Zirconium tetraiodide (Aldrich) and trimethylphosphine (Aldrich) were used as received. Tri-*tert*-butylsilanol[28] and $TiCl_4(THF)_2$[34] were prepared by literature procedures. Nitriles and isonitriles were distilled and then vacuum transferred from activated 4-Å molecular sieves. Ammonia (Matheson, anhydrous grade) was dried over Na^0 and vacuum transferred prior to use. Acetone and acetaldehyde were distilled from K_2CO_3 and then vacuum transferred from activated 4-Å molecular sieves. Benzophenone (Fisher) and 4,4′-dimethylbenzophenone (Lancaster) were sublimed before use. Benzophenone-d_{10} (Cambridge) was used as received. All other ketones and aldehydes used in EPR studies were used as received.

Routine ^1H and $^{13}C\{^1H\}$ NMR spectra were recorded on a Varian XL-200 or a Varian XL-400 spectrometer and referenced to the residual solvent peak. EPR spectra were obtained on a Bruker ER 200D instrument using a NMR ER 035M gaussmeter and Varian frequency counter to calculate g values. Low temperatures were maintained and monitored using a Varian Instruments variable-temperature controller. Powder spectra were obtained in a 2-methylpentane glass with the sample tube immersed in a liquid-nitrogen-filled EPR probe. UV–visible spectra were recorded on an HP 8531 diode-array spectrophotometer. Infrared spectra were recorded as Nujol mulls on a Mattson FT-IR instrument interfaced to an AT&T PC7300 computer. Magnetic susceptibilities were determined by the Evan's method in benzene-d_6 using a NMR tube coaxial insert (Wilmad). Molecular weights were determined by cryoscopy in benzene using a locally made device. Analyses were performed by Analytische Laboratorien, Elbach, Germany, and Oneida Research Services, Whitesboro, NY.

Procedures. 1. Na(silox). To a flask charged with (silox)H (11.0 g, 51 mmol) and Na^0 (1.60 g, 70 mmol) was added 60 mL of hexanes at −78 °C. The solution was warmed to 23 °C under Ar and then refluxed for 10 h with evolution of H_2. The solution was then degassed and filtered. Concentration of the filtrate and cooling to −78 °C yielded Na(silox) as a white crystalline solid (9.8 g, 82%). ^1H NMR (C_6D_6): δ 1.18 (CH_3). $^{13}C\{^1H\}$ (C_6D_6): δ 23.40 ($SiCCH_3$), 31.63 ($SiCCH_3$). This preparation gives a higher yield and purity than the previously reported preparation with NaH in THF.[29]

2. $(silox)_3TiCl$ (1). To a flask containing $TiCl_4(THF)_2$ (3.73 g, 11.2 mmol) and Na(silox) (8.00 g, 33.6 mmol) was added 60 mL of THF at −78 °C. When warmed to room temperature, the yellow solution faded to cloudy white. This solution was then refluxed for ~12 h. After cooling, the THF was removed, and the white solid was triturated twice with 30 mL of hexanes. After filtration, concentration and cooling of the filtrate to −78 °C yielded colorless, crystalline **1** (6.95 g, 85%). ^1H NMR (C_6D_6): δ 1.30 (CH_3). $^{13}C\{^1H\}$ NMR (C_6D_6): δ 23.98 (SiC), 30.80 (CH_3). IR (Nujol, cm^{-1}): 970 (w), 935 (w), 890 (w), 860 (s), 815 (m), 750 (w), 635 (s). Anal. Calcd for $C_{36}H_{81}Si_3O_3TiCl$: C, 59.26; H, 11.19. Found: C, 59.12; H, 11.10.

3. $(silox)_3ZrCl$ (2). To a flask charged with $ZrCl_4$ (1.00 g, 4.19 mmol) and Na(silox) (3.00 g, 12.59 mmol) was added THF at −78 °C. The solution was slowly warmed to 23 °C and allowed to stir for ~12 h. The THF was removed and replaced with hexanes. After filtration, concentration of the filtrate to <10 mL followed by cooling to −78 °C provided colorless, crystalline **2** (2.20 g, 68%). ^1H NMR (C_6D_6): δ 1.24 (CH_3). $^{13}C\{^1H\}$ (C_6D_6): δ 23.23 ($SiCCH_3$), 30.51 ($SiCCH_3$). Anal. Calcd for $C_{36}H_{81}Si_3O_3ZrCl$: C, 55.94; H, 10.56. Found: C, 55.77; H, 10.56.

4. $(silox)_3ZrI$ (3). To a flask charged with ZrI_4 (1.67 g, 2.79 mmol) and Na(silox) (2.01 g, 8,44 mmol) was added THF at −78 °C. The solution was warmed to 23 °C and then brought to reflux for 10 h. The THF was removed and replaced with hexanes. After filtration, concentration of the filtrate to <10 mL followed by cooling to −78 °C provided colorless, crystalline **3** (1.56 g, 65%). ^1H NMR (C_6D_6): δ 1.25 (CH_3). $^{13}C\{^1H\}$ (C_6D_6): δ 23.09 ($SiCCH_3$), 30.59 ($SiCCH_3$).

5. $(silox)_3Ti$ (4). To a flask containing freshly prepared Na/Hg amalgam, $(silox)_3TiCl$ (**1**, 2.71 g, 3.71 mmol), and a glass-encased stir bar was added 60 mL of DME. On warming, the solution turned faint green due to presence of $(silox)_3Ti(DME)$ (**4**–DME) and rapidly darkened. After the solution was stirred for 6 h, the DME was removed from the greenish brown solution. Toluene (~30 mL) was repeatedly added and then removed until the green color was absent in the solid. Hexanes (~40 mL) were added and the solution was filtered, concentrated, and cooled to −78 °C, yielding bright orange, crystalline **4** (1.96 g, 76%). ^1H NMR (C_6D_6): δ 1.50 (CH_3, s, $\upsilon_{1/2}$ = 110 Hz). UV–vis [hexane; λ, nm (ϵ, M^{-1} cm^{-1})]: 211 (15 000), 248 (13 600), 500 (360). M_r: found, 709 (calcd, 694). Anal. Calcd for $C_{36}H_{81}Si_3O_3Ti$: C, 62.29; H, 11.76. Found: C, 62.02; H, 11.58.

6. $(silox)_3Ti(L)$ (4–L). To a flask charged with $(silox)_3Ti$ (**4**) (0.500 g, 0.72 mmol) and 5 mL of pentane at −78 °C was added a ligand (L = DME, PMe_3, CNMe, CN^{t}Bu, NC^{t}Bu, NH_3) via a calibrated gas bulb. The orange solution turned green on warming. Cooling the solution to −78 °C, followed by the slow removal of some pentane, resulted in the crystallization of the adducts. (yields 55–76%). All of these complexes

(79) Ziebarth, M.; Neumann, W. P. *Liebigs Ann. Chem.* **1978**, 1765–1774.
(80) Neumann, W. P.; Schroeder, B.; Ziebarth, M. *Liebigs Ann. Chem.* **1975**, 2279–2292.

will lose the coordinated ligand under vacuum or upon heating; only **4**–CNR complexes were stable enough for elemental analysis. They were stored in a −25 °C refrigerator in the drybox.

(a) 4–DME. ^{1}H NMR [C_6D_6; δ ($\upsilon_{1/2}$ (Hz), assignment)]: 1.5 (110, silox), 3.6 (28, OCH_3), 3.8 (35, OCH_2). Significant dissociation to **4** and DME was observed.

(b) 4–CNMe. ^{1}H NMR [C_6D_6; δ ($\upsilon_{1/2}$ (Hz), assignment)]: 1.4 (30, silox), 55 (480, NCH_3). UV–vis [hexane; λ, nm (ϵ, M^{-1} cm^{-1})]: 270 (4530), 382 (1590). IR (Nujol, cm^{-1}): 2209, ν(CN). Anal. Calcd for $C_{38}H_{84}Si_3O_3NTi$: C, 62.08; H, 11.52; N, 1.91. Found: C, 61.81; H, 11.36; N, 2.02.

(c) 4–CN^{t}Bu. ^{1}H NMR [C_6D_6; δ ($\upsilon_{1/2}$ (Hz), assignment)]: 1.4 (35, silox), 2.8 (15, $C(CH_3)_3$). IR (Nujol, cm^{-1}): 2250, ν(CN).

(d) 4–NC^{t}Bu. ^{1}H NMR [C_6D_6; δ ($\upsilon_{1/2}$ Hz); assignment)]: 1.4 (46, silox), 3.5 (36, $C(CH_3)_3$). IR (Nujol, cm^{-1}): 2246, ν(NC).

(e) 4–PMe$_3$. ^{1}H NMR [C_6D_6; δ($\upsilon_{1/2}$ (Hz), assignment)]: 1.2 (40, silox); PCH_3 not observed, but excess PMe_3 was present in order for the equilibrium to be favorable for the adduct.

(f) 4–NH$_3$. To an NMR tube was added (silox)$_3$Ti (**4**; 23 mg, 0.033 mmol) and 0.5 mL of C_6D_6. The solution was freeze–pump–thaw degassed three times, and then NH_3 (0.33 mmol) was admitted via a calibrated gas bulb and condensed into the tube at 77 K. The tube was sealed under vacuum. On shaking and thawing, the clear orange solution turned a light blue. **4**–NH_3 is unstable with respect to loss of ammine in the absence of excess ammonia, thus scaleup and isolation were not attempted. ^{1}H NMR [C_6D_6; δ ($\upsilon_{1/2}$ (Hz), assignment)]: 1.2 (25, silox), 125 (1600, NH_3).

7. (silox)$_3$Ti(OCMe$_2$H) (5a) + (silox)$_3$Ti(OCMe=CH$_2$) (6a). To a flask containing (silox)$_3$Ti (**4**; 25 mg, 0.036 mmol) and 5 mL of hexanes at 23 °C was added acetone (0.037 mmol) by calibrated gas bulb. The solution quickly bleached from a bright orange to a pale yellow. The solvent was stripped, and the residue was analyzed by ^{1}H NMR spectroscopy. The two products proved inseparable on scaleup. (silox)$_3$Ti(OCMe$_2$H) (**5a**): ^{1}H NMR (C_6D_6) δ 1.29 ($OCH(CH_3)_2$, br, partially obscured by silox), 1.299 (silox, s, 81 H), 4.79 ($OCHMe_2$, septet, 1 H, J = 6 Hz); $^{13}C\{^1H\}$ (C_6D_6) δ 23.57 ($SiCCH_3$), 26.29 ($OCH(CH_3)_2$), 30.91 ($SiCCH_3$), 81.39 (OC). (silox)$_3$Ti(OCMe=CH$_2$) (**6a**): ^{1}H NMR (C_6D_6) δ 1.31 (silox, s, 81 H), 1.85 ($OC(CH_3)$, s, 3 H), 4.16 ($OCHH$, s, 1, H), 4.62 ($OCHH$, s, 1 H); $^{13}C\{^1H\}$ (C_6D_6) δ 22.76 ($OC(CH_3)$), 23.61 ($SiCCH_3$), 30.99 ($SiCCH_3$), 93.61 ($OC=CH_2$), 165.79 (OC).

8. (silox)$_3$Ti(OEt) (5b) + (silox)$_3$Ti(OCH=CH$_2$) (6b). To a flask containing (silox)$_3$Ti (**4**; 28 mg, 0.040 mmol) and 5 mL of hexanes at 23 °C was added acetaldehyde (0.041 mmol) by calibrated gas bulb. The bright orange solution turned colorless and then developed a slight yellow tinge. The solvent was stripped and the residue analyzed by ^{1}H NMR spectroscopy. The two products proved inseparable on scaleup. (silox)$_3$Ti(OEt) (**5b**): ^{1}H NMR (C_6D_6) δ 1.17 (OCH_2CH_3, t, 3 H, J = 7 Hz), 1.295 (silox, s, 81 H), 4.40 (OCH_2CH_3, q, 2 H, J = 7 Hz); $^{13}C\{^1H\}$ (C_6D_6) δ 23.56 ($SiCCH_3$), 29.82 (OCH_2CH_3), 30.88 ($SiCCH_3$), 74.37 (OCH_2CH_3). (silox)$_3$Ti(OCH=CH$_2$) (**6b**): ^{1}H NMR (C_6D_6) δ 1.300 (silox, s, 81 H), 4.08 (OC(H)=CHH^t, d, 1 H, J = 5.6 Hz), 4.59 (OC(H)=CHH^t, d, 1 H, J = 13.4 Hz), 7.08 (OC(H)=CHH^t, dd, 1 H, J = 7 Hz, 13.4 Hz); $^{13}C\{^1H\}$ (C_6D_6): δ 23.59 ($SiCCH_3$), 30.90 ($SiCCH_3$), 94.39 ($OC=CH_2$), 156.45 ($OCH(CH_3)_2$).

9. EPR Studies of (silox)$_3$Ti(OCRR′•) (4-OCRR′). To an EPR tube containing 3–5 mg (silox)$_3$Ti (**4**) were added a hydrocarbon solvent (typically toluene, hexane, or 2-methylpentane) and varying amounts of the ketone/aldehyde of interest. In the case of **4**–$OCPh_2$, a small quantity of **7** (~10 mg) was used. The samples were then capped and cooled in the EPR cavity.

10. [(silox)$_3$Ti(OCPh$_2$)]$_2$ (7). To a flask containing (silox)$_3$Ti (**4**; 500 mg, 0.72 mmol) and freshly sublimed benzophenone (131 mg, 0.72 mmol) was added 25 mL of hexane at −78 °C. When warmed to 23 °C, the solution turned a deep red and then faded to yellow. Concentration of the hexane solution yielded **7** as a yellow powder which was isolated by filtration at room temperature (416 mg, 66%). ^{1}H NMR [C_6D_6, 0.011 M, 21 °C (tentative assignments)]: δ 1.25 (silox, s, 162 H), 4.81 ((=CH)$_2$(CH)C, m, 1 H), 5.40, 6.02, 6.51, (=CH–, br d, 1 H each, J ~ 10 Hz), 7.43 (=CH–, br d, 1 H, J ~ 10 Hz), 6.9–7.6, 7.8–8.0 (Ph, m, 15 H). $^{13}C\{^1H\}$ [THF-d_8 (tentative assignments)]: δ 24.26, 24.16 ($SiCCH_3$), 31.66, 31.39 ($SiCCH_3$), 55.09 (allylic), 99.79 ($OCPh_2R$), 116.93, 124.68, 125.30, 125.42 (olefinic), 127–132 (multiple Ph), 137.71, 143.94, 147.08 (C_{ipso}), 163.06, 167.00 (C=C(Ph)O). The above chemical shifts are concentration and temperature dependent. Anal. Calcd for $C_{98}H_{182}Si_6O_8Ti_2$: C, 67.15; H, 10.47. Found: C, 66.98; H, 10.33.

11. (silox)$_3$TiOCHPh$_2$ (8). To a flask containing [(silox)$_3$Ti(OCPh$_2$)]$_2$ (**7**; 400 mg, 0.23 mmol) and Ph_3SnH (277 mg, 0.79 mmol) was added 15 mL of benzene. The solution was stirred at room temperature for 4 h. The benzene was removed and replaced with hexanes. After filtration, concentration of the filtrate and cooling to −78 °C yielded light yellow microcrystals of **8** (183 mg, 45%). ^{1}H NMR (C_6D_6): δ 1.26 (silox, s, 81 H), 6.78 (OCH, s, 1 H) 7.0–7.6, 8.0–8.2 (Ph, m, 10 H). $^{13}C\{^1H\}$ (C_6D_6): δ 23.48 (SiC), 30.95 (CH_3), 91.47 (OC), 126.19 (C_{ortho}), 127.57 (C_{para}), 128.60 (C_{meta}), 146.20 (C_{ipso}). Anal. Calcd for $C_{49}H_{92}Si_3O_4Ti$: C, 67.08; H, 10.57. Found: C, 67.02; H, 10.37.

12. Equilibrium Studies of 7 ⇌ 2(4–OCPh$_2$•). Solutions of [(silox)$_3$Ti(OCPh$_2$)]$_2$ (**7**) of known concentration (4.4×10^{-4}, 2.2×10^{-3}, and 1.1×10^{-3} M in hexanes) were prepared in volummetric flasks. A 5-mL aliquot of one solution was then added to a modified UV–vis cell, consisting of a quartz cell, an adjoining Pyrex bulb, and a needle valve. The solution was degassed in the Pyrex bulb, then placed under 300 Torr of argon to minimize vacuum transfer of the solvent, and poured into the quartz cell. The cell was immersed in the constant-temperature tank of a circulating bath for 10 min to reach thermal equilibrium, vigorously shaken to assure complete mixing, and then removed from the bath, wiped off, and placed in a variable-temperature UV–vis cell holder served by the same circulating bath. Two spectra were taken in this way (the cell returned to the tank after each spectrum), and the average absorbance between 644 and 648 nm was determined. This averaged absorbance and a molar absorptivity of 1800 M^{-1} cm^{-1} were used to calculate the equilibrium concentration of **4**–$OCPh_2$. The concentration of **7** was calculated using conservation of matter, and equilibrium constants were determined for 11–12 temperatures between 24 and 86 °C. Above 86 °C, vacuum transfer of solvent from the UV–vis cell to the cooler portions of the inert atmosphere cell was a significant problem. A plot of ln K vs $1/T$ was linear ($R^2 > 0.99$) for each of the three concentrations. Addition of a 10-fold excess of benzophenone or a change to toluene as the solvent had little effect on the equilibrium constants or the thermodynamic parameters.

13. Electrochemistry. In an inert-atmosphere glovebox, solutions were prepared with 1 mM sample and 0.10 M ^{n}Bu$_4$NBF$_4$ in THF. Three electrodes, consisting of a 0.03-in-diameter Pt working electrode, a Ag/AgCl pseudoreference electrode, and a Pt auxiliary electrode were placed in the unstirred solution. After cyclic voltammograms (CV's) of the sample were recorded, ferrocene was added as an internal reference and the CV's were measured again. Potentials are reported vs Ag/AgCl in THF and are uncorrected.

Acknowledgment. Primary support from the Air Force Office of Scientific Research (AFOSR-87-0103) and the National Science Foundation (CHE-8714146) is gratefully acknowledged, as are contributions from the Union Carbide Innovation Recognition Program and Cornell University. We are grateful to Prof. Frank Feher and co-workers S. Wells and J. Hemminger for allowing disclosure of their XPS results. Dr. George Parshall, Dr. Steve Ittel, and the Central Research & Development Department of E. I. du Pont de Nemours & Co., Inc. are thanked for hosting and supporting P.T.W. during a sabbatical leave. We also thank Drs. Ralph Wheeler and Marjanne Zonnevylle for EHMO calculations and Prof. Barry K. Carpenter, Prof. Robert Scott, and Dr. David Budil for helpful discussions. Support for the Cornell NMR Facility from the NIH and NSF Instrumentation Programs is acknowledged.